Rivista Italiana di Paleontologia e Stratigrafia
(*Research in Paleontology and Stratigraphy*)
vol. 127(3): 557-583. **November 2021**

USING HIGH-RESOLUTION AMMONITE BIOCHRONOSTRATIGRAPHY TO DATE VOLCANOGENIC DEPOSITS PRESERVED IN MIDDLE JURASSIC CARBONATE PLATFORMS SUCCESSIONS OF THE WESTERNMOST TETHYS (SOUTHEASTERN IBERIAN RANGE, SPAIN)

JOSÉ EMILIO CORTÉS

Departamento de Geodinámica, Estratigrafía y Paleontología, Facultad de Ciencias Geológicas, Universidad Complutense de Madrid. José Antonio Novais 12, 28040 Madrid, Spain. E-mail: jocortes@ucm.es

To cite this article: Cortés J.E. (2021) - Using high-resolution ammonite biochronostratigraphy to date volcanogenic deposits preserved in Middle Jurassic carbonate platforms successions of the westernmost Tethys (southeastern Iberian Range, Spain). *Riv. It. Paleontol. Strat.,* 127(3): 557-583.

Keywords: Ammonite associations; biochronostratigraphy; Jurassic Alpine Ocean; intracontinental volcanism.

Abstract. The Middle Jurassic successions that are currently exposed in eastern Spain (southeastern Iberian Range) were deposited in a system of shallow carbonate platforms, constituting the western margin of the Alpine Ocean, and display a series of successively interbedded volcaniclastic rocks and minor lava flows. The large-scale mapping reveals that Middle Jurassic volcanic rocks crop out along NW-SE pathways, highlighting the importance of the role played by tectonics in controlling the spatial distribution of volcanic outcrops. The progressive dismemberment of Pangea impelled a geographic provinciality increase and, thus, might have contributed to a growing speciation rate of marine invertebrate organisms, notably ammonites. The present study provides new data constraining in detail the age of the Middle Jurassic volcanic deposits. The biochronostratigraphic calibrations of the sedimentary host rocks encasing the volcanics have been obtained from the study of the fossil content (mainly ammonites) from16 well-exposed stratigraphic sections. The study of the fossils from these sections has enabled the identification of three volcanic episodes during the Murchisonae Zone (Aalenian), the Concavum-Discites zonal boundary (Aalenian-Bajocian), and the late Laeviuscula Zone or Laeviuscula-Propinquans zonal boundary (Bajocian). Precise age constraints for volcanic accumulations can be a significant contribution in reconstructing the geodynamic history of the Iberian Basin.

Introduction

During the time interval spanning from the late Pliensbachian to the Tithonian, an extensional episode that coincided with the production of oceanic crust developed in the westernmost Tethys realm. The opening of the Central Atlantic did not continue northwards but was exported to the east through the Gibraltar Fault in the Pliensbachian, leading to the formation of the Alpine mid-ocean ridge (Schettino & Turco 2011).

Received: December 31, 2020; accepted: June 26, 2021

The simultaneous presence of synsedimentary active faults with an associated coeval volcanism in the eastern (e.g., Cortés 2018, 2020a) and southern (e.g., Puga et al. 2004; Vera et al. 2004; Gómez et al. 2019) Iberian paleomargins indicates that the magmatic events that were linked to the Alpine mid-ocean-ridge areas affected wider regions. Lower and Middle Jurassic volcanic deposits, represented by basaltic rocks with an alkaline affinity (Ancochea et al. 1988; Lago et al. 2004), appear interbedded in the shallow-marine sediments from the southeastern Iberian Range. Reports of their existence range from the 1930s (Bakx 1935; Martin 1936), passing

through the 60s, 70s, 80s and 90s (Gautier 1968; Ortí & Sanfeliu 1971; Gómez et al. 1976; Gómez & Goy 1977; Gómez 1979; Ortí & Vaquer 1980; Fernández-López et al. 1985; Gautier & Odin 1985; Ortí 1987; Ancochea et al. 1988; Odin et al. 1988; Lago et al. 1996; Martínez et al. 1996a,b,c,d, 1997a,b, 1998; Martínez-González et al. 1996; Valenzuela et al. 1996) until the last years (Palencia et al. 2000; Palencia-Ortas 2000; Lago et al. 2004; García-Frank 2006; García-Frank et al. 2006, 2008; de Santisteban 2016, 2018; Cortés & Gómez 2016, 2018; Cortés 2018, 2020a,b).

The quantification and precise dating of these volcanic deposits could contribute to the reconstruction of the geodynamic evolution of the paleogeographic setting in question. For this purpose, Gautier & Odin (1985) and Odin et al. (1988) implemented absolute age determinations by radiometric methods, but their results were unsatisfactory, since the ages obtained were much more recent than it would have been expected from the stratigraphic setting. However, the fossil-record richness of the Lower and Middle Jurassic sediments provided an opportunity to date their interbedded volcanic accumulations. Lower and Middle Jurassic times recorded significant peaks in the ammonite diversification. Thus, since ammonites show rapid rates of speciation and extinction, broad geographic distributions, and well-established chronostratigraphic frameworks (Neige & Rouget 2015), high-resolution ammonite biostratigraphy turned out to be an efficient and powerful tool for dating and correlation in the marine sedimentary successions of the studied area. Taxonomic analyses of other fossil groups, such as brachiopods, provided additional data for checking and refining the sediment ages, and have become an alternative help when there are no ammonites available.

Cortés (2018) was the first to identify 13 volcanic phases within a period spanning from the early Pliensbachian to the early Bajocian. The present work aims to raise knowledge about the spatial and temporal frame of the three youngest volcanic episodes included within the Middle Jurassic lithostratigraphic units. This currently accessible information on the quantification and the precise age of volcanics contributes to the reconstruction of the geological history and the geodynamic evolution of the eastern Iberian paleomargin in the western Tethys during Jurassic times. Moreover, it might provide the basis for further regional research works in other disciplines such as paleomagnetic or geochemical studies.

Geological Setting

It can be defined a complete Wilson Cycle (the Alpine Cycle) from the beginning of the rifting events leading to the break-up of Pangea (late Permian-Lower Cretaceous) until the end of the convergence and collision of the northward-moving African, Arabian, and Indian plates with the Eurasian plate (from the latest Cretaceous to the present), which, in turn, was preceded by another Wilson Cycle (the Variscan Cycle) (Quesada & Oliveira 2019). The Alpine Cycle in Iberia started with a set of Permo-Triassic rift systems formed to the northeast and southeast of Iberia, around the uplifted and emerged Iberian Massif. The geometry of these intracratonic basins was strongly influenced by inherited ancient Variscan structures, many of which were reactivated repeatedly either as normal faulting through the extensional stage (Alpine pre-orogeny) or as reverse faulting during the subsequent tectonic inversion that occurred in the orogenic phase (Vergés et al. 2019). One of those Alpine intracratonic basins was the Iberian Basin, which became a carbonate-platform system to constitute the eastern paleomargin of Iberia in Jurassic times (Gómez et al. 2004), and which, during the Cenozoic compressive events, gave rise to the current Iberian Range (Vegas et al. 2019). The Iberian Range runs northwest-southeast for over 500 km in central-eastern Spain and is an integral part of the Alpine-Himalayan orogenic belt that stretches along the southern Eurasian margin as a consequence of the mentioned plate collision during the Alpine orogeny. The studied area is located in the southeastern part of the Iberian Range, where its Castilian-Valencian and Aragonese branches converge (Fig. 1A).

In the studied area, the present-day Lower and Middle Jurassic outcrops were deposited in shallow marine settings emplaced onto the eastern paleomargin of Iberia at 30-35ºN (Osete et al. 2011) (Fig. 1B). When this happened, Iberia underwent the first pre-orogenic passive margin stage of the Alpine Cycle, from the latest Triassic to the Middle-Upper Jurassic boundary, according to Gómez et al. (2019). Contrasting with the tectonically quiet pe-

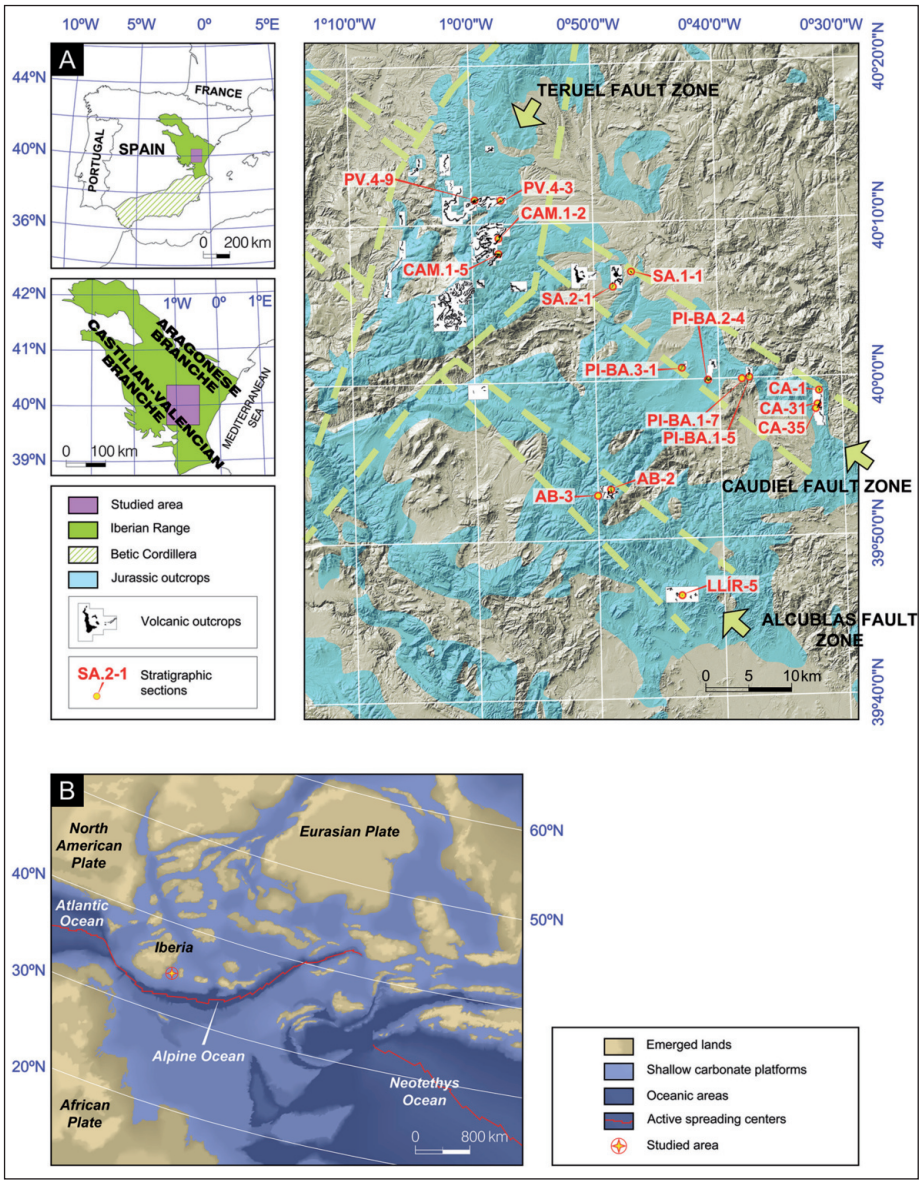

Fig. 1 - Location of the studied area. A) Ubication of outcropping volcanic rocks and stratigraphic sections along the Caudiel, Alcublas, and Teruel fault zones. B) Middle Jurassic paleogeographic reconstruction of the western Tethys with the indication of the studied area in the Iberian eastern paleomargin (modified from Schettino and Turco 2011, and Blakey 2011. Paleolatitudes adapted from Osete et al. 2011).

riods predicted by the thermal subsidence model, Fernández-López & Gómez (2004) and Gómez & Goy (2005) pointed out that a grid of NW-SE and NE-SW trending active normal faults developed in the east margin of Iberia throughout the Lower and Middle Jurassic. The faulting network brought synsedimentary block tectonics that underwent differential subsidence and resulted in a variation in thickness and lithologies. In addition, it can be noted that the outcrops of volcanic rocks are aligned along three of these faults: the Teruel, Caudiel, and Alcublas faults or, more appropriately, fault zones (Fig. 1A).

Despite an undeniable tectonic control, the high-rank transgressive and regressive sedimentary conditions recorded across the eastern Iberian platform system also indicate an eustatic forcing influence. Identifying major discontinuities of regional extent which represent noteworthy time gaps combined with facies stacking pattern analyses may allow the recognition of high-rank cycles (first- and second-order cycles). Two regionally extensive gaps in the stratigraphic record occurred at the scale of the whole Iberian platform system, one during the lower part of the Aalenian Murchisonae Zone (Fernández-López 1997; Fernández-López & Gómez 2004; Gómez & Fernández-López 2004, 2006; Gómez et al. 2004) and the other at the Middle-Upper Jurassic boundary (e.g., Bulard 1971; Fernández-López & Gómez 2004). Thus, except for the earliest Aalenian deposits, the rest of the Middle Jurassic succession (from the middle Murchisonae Aalenian Zone until the upper Callovian) represents a first-order cycle, the Middle Jurassic major T-R

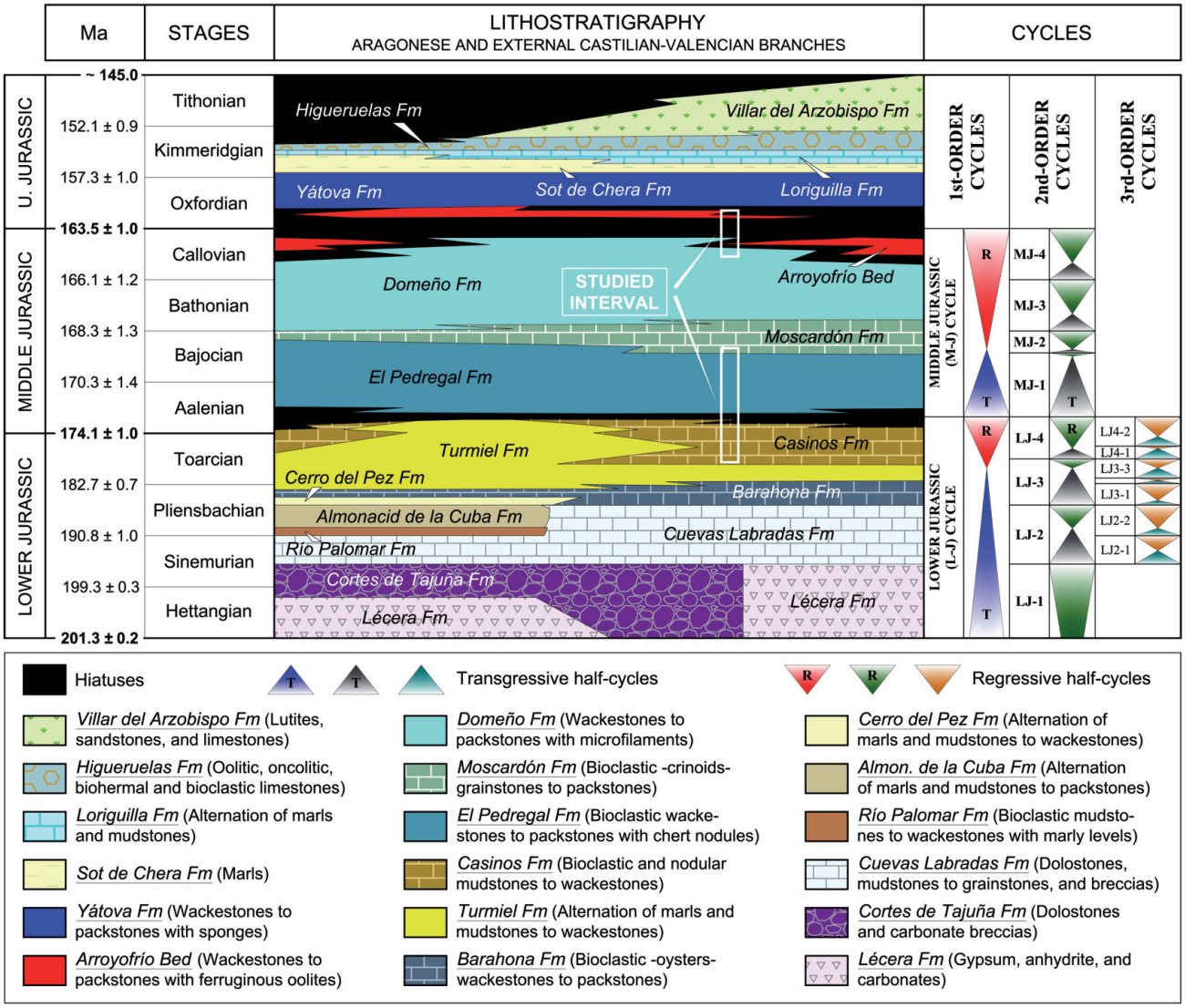

Fig. 2 - Synthetic chronostratigraphic chart showing the Lower and Middle Jurassic lithostratigraphic units and the sedimentary cyclicity across the Aragonese and Castilian-Valencian branches of the Iberian Range (adapted from Gómez et al. 2004 and Aurell et al. 2019), together with the specification of the studied interval. The time scale used is that of the Chronostratigraphic Chart (2021) (Cohen et al. 2013; updated).

cycle of Aurell et al. (2003). The development of expanded sections with marly deposits representative of open-marine environments, supported with ammonite taphonomic analyses, have led to the detection of the major flooding (peak transgression) at the upper Niortense Bajocian Zone throughout this first-order cycle (Fernández-López 1997; Aurell et al. 2003).

Four second-order transgressive-regressive cycles, named MJ-1, MJ-2, MJ-3, and MJ-4, have been identified within the Middle Jurassic first-order cycle. The MJ-1 Cycle is strongly asymmetric and displays a transgressive unit ranging from the Aalenian (Murchizonae Zone) to the lower Bajocian Humphriesianum Zone, where the transgressive peak is recorded. The regressive episode develops entirely within the Humphriesianum Zone, with its top coinciding with the boundary between the Humphriesianum and Niortense zones (Gómez et al. 2004). This cycle is represented by the El Pedregal Formation (Gómez et al. 2004), except in the Caudiel outcrop, where the Moscardón Formation can appear locally towards the end of the cycle closely linked to the volcanic mound and topographic highs (Cortés 2020b).

The MJ-2 Cycle starts together with the Niortense Zone and ends up in the Bajocian-Bathonian boundary (Parkinsoni-Zigzag zonal limit). The major marine transgression matches that of the first-order cycle in the Niortense Zone. The El Pedregal Formation is involved at the beginning and the middle of

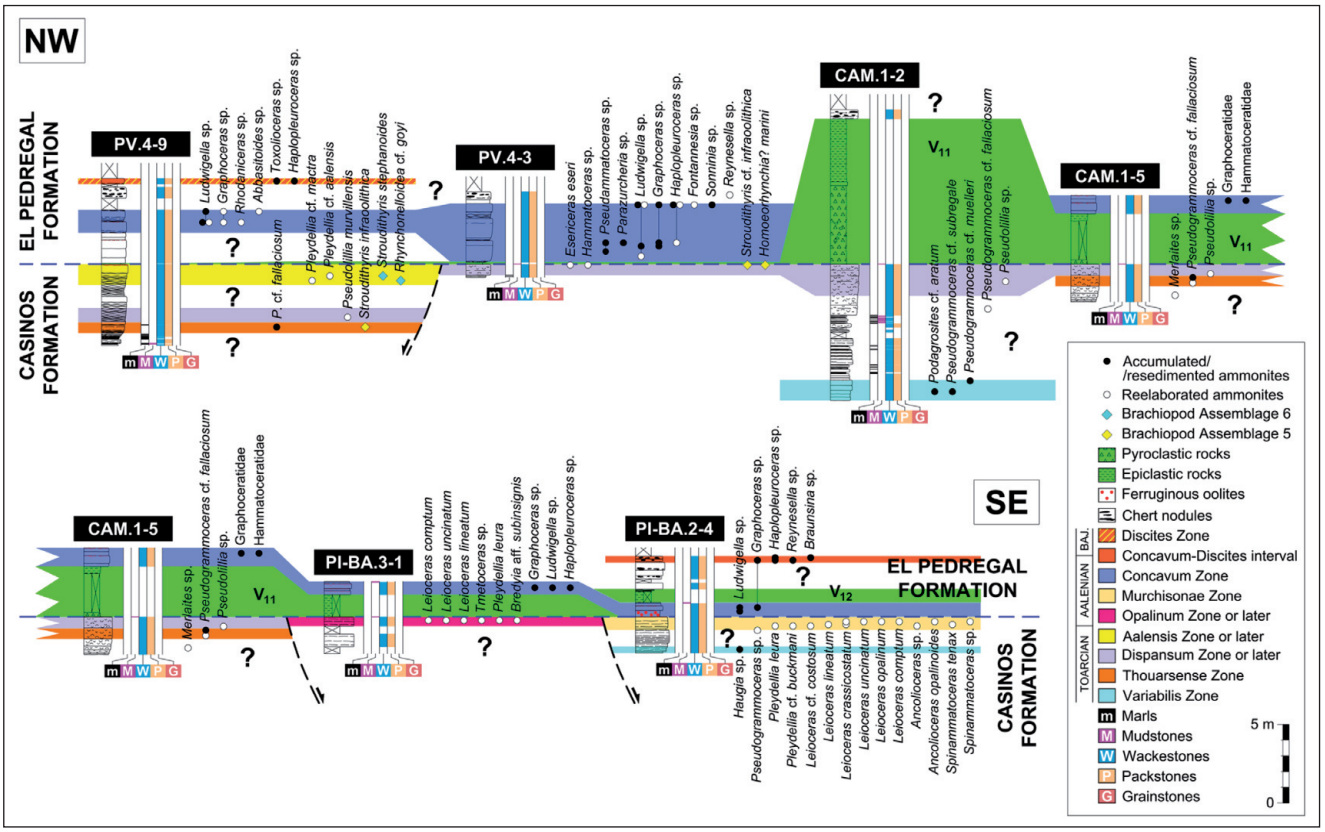

Fig. 3 - Graphic representation of the PV.4-9, PV.4-3, CAM.1-2, CAM.1-5 (Teruel Fault Zone), PI-BA.3-1, and PI-BA.2-4 (Caudiel Fault Zone) stratigraphic sections, showing the chronostratigraphic position of the volcanic episode V_{11}, and of the volcanic episode V_{12} in the PI-BA.2-4 log, together with the variations in the age of the lithostratigraphic units immediately below the volcanic levels from northeastern to southeastern outcrops.

the cycle, whereas the Moscardón Formation appears at the end (Gómez et al. 2004).

The MJ-3 Cycle coincides with the Bathonian boundaries, the maximum flooding events being achieved in the Subcontractus Zone. The created accommodation is usually filled with sediments belonging to the lower part of the Domeño Formation (Gómez et al. 2004). However, in southeastern areas such as the Caudiel outcrop, the Moscardón Formation shows at early stages (Zigzag Zone) of the cycle (Fernández-López et al. 1985; Fernández-López 1986; Cortés 2018, 2020b).

The MJ-4 Cycle ranges throughout the entire Callovian, with the maximum flooding peak located in the Gracilis Zone. The Domeño Formation (upper part) and the Arroyofrío Bed (p.p.) at its top characterize the sedimentation during this cycle. A widespread regional hiatus affects, at least, the Lamberti Zone (Gómez et al. 2004).

The spatio-temporal relationships among the lithostratigraphic units, together with their correlation with transgressive-regressive cycles, are illustrated in the synthetic chronostratigraphic chart in Fig. 2.

Materials and methods

Sixteen highly ammonite-rich stratigraphic sections containing the best exposed volcanic deposits (stratigraphically located in the lower part of the El Pedregal Formation, above the top of the Casinos Formation) have been measured, logged, and paleontologically sampled in order to date, as accurately as possible, the Middle Jurassic volcanics. The relative age of the volcanic phases has been obtained by biochronostratigraphic dating methods applied directly on the encasing fossiliferous sediments, whose ammonite content have yielded very refined calibrations at the zone scale.

The taphonomic states of ammonites were distinguished following the diagnostic criteria of Fernández-López (1984a,b) to identify reelaborated elements. In this work, the letter (r) indicates both the accumulated specimens (i.e., elements that have been settled on the seafloor and have not undergone movement either before or after the burial) and the resedimented ones (i.e., those that, after their accumulation, have been moved -rolling and tumbling, usually generating broken shells- on the sedimentary surface before burial, but not afterward). The letter (w) designates the reelaborated specimens, previously buried, that were exhumed from older sediments, developing abrasion and disarticulation surfaces, coating, several phases of cementation and sedimentary filling, as well as traces of bioerosion and encrustation, among others, before their final burial. The internal molds of both accumulated and resedimented elements are similar in texture and coeval to the sedimentary rocks in which they are included. By contrast, the reworked internal molds show petrologic differences and discontinuity with the sedimentary matrix.

Stratigraphic sections	Geographic coordinates	Lithostratigraphic units	Volcanic episodes
CA-1	39º59'17.84"N, 0º31'46.82"W	El Pedregal Fm	V_{12}
CA-31	39º58'15.50"N, 0º31'50.81"W	El Pedregal Fm	V_{12}
CA-35	39º58'08.95"N, 0º31'54.76"W	El Pedregal Fm	V_{12}
PI-BA.1-5	40º00'09.18"N, 0º37'30.75"W	El Pedregal Fm	V_{12}
PI-BA.1-7	40º00'05.82"N, 0º37'53.92"W	El Pedregal Fm	V_{12}
PI-BA.2-4	40º00'00.10"N, 0º40'48.92"W	El Pedregal Fm	V_{12}
PI-BA.3-1	40º00'49.66"N, 0º42'55.23"W	Casinos Fm/El Pedregal Fm	V_{11}
SA.1-1	40º06'54.10"N, 0º46'55.45"W	El Pedregal Fm	V_{12}
SA.2-1	40º05'54.21"N, 0º48'31.41"W	El Pedregal Fm	V_{12}
LLÍR-5	39º46'30.53"N, 0º43'17.69"W	El Pedregal Fm	V_{13}
AB-2	39º53'13.39"N, 0º48'55.59"W	El Pedregal Fm	V_{13}
AB-3	39º52'45.79"N, 0º49'55.48"W	El Pedregal Fm	V_{13}
PV.4-3	40º11'35.00"N, 0º57'26.13"W	Casinos Fm/El Pedregal Fm	V_{11}
PV.4-9	40º11'34.90"N, 0º59'43.80"W	Casinos Fm/El Pedregal Fm	V_{11}
CAM.1-2	40º09'09.82"N, 0º57'37.72"W	Casinos Fm/El Pedregal Fm	V_{11}
CAM.1-5	40º08'11.61"N, 0º57'36.47"W	Casinos Fm/El Pedregal Fm	V_{11}

Tab. 1 - Main data of the stratigraphic sections (geographic coordinates, lithostratigraphic units, and volcanic episodes contained).

Their age can be either apparently synchronous (within the limits of biochronostratigraphic resolution) or older than the enclosing rocks.

The ammonite zones used here for the late Toarcian are the "Standard Zones" of Page (2003) for the Northwest European Province. The zonation of the Aalenian and Bajocian stages reproduces the biochronostratigraphic scheme presented by Fernández-López (1985) and Pavia & Fernández-López (2016, 2019) for the Mediterranean-Caucasian Subrealm. The brachiopod fauna has been included in the assemblages 5 and 6 established by García Joral & Goy (2000), García Joral et al. (2011), and Baeza-Carratalá et al. (2016). The Lower and Middle Jurassic transgressive-regressive facies cycles of third, second, and first order employed in this work are those established by Gómez & Goy (2000, 2005), Aurell et al. (2003), and Gómez et al. (2004).

Results

The Jurassic volcanic outcrops in the southeastern Iberian Range are aligned along three structural pathways (fault zones). Two of them, the Caudiel and the Alcublas fault zones, show a NW-SE trend, while the third, the Teruel Fault Zone, follow a NE-SW or NNE-SSW direction (Gómez & Goy 2005; Gómez & Fernández-López 2006; Cortés 2018, 2020a,b). Although the Lower Jurassic volcanic outcrops are grouped around the Teruel Fault Zone, with occasional incursions towards the Caudiel Fault Zone, the Middle Jurassic volcanic outcrops are strongly clustered around the Caudiel and the Alcublas fault zones, with some vestigial appearances in the Teruel Fault Zone (Cortés 2018, 2020a,b).

Sixteen stratigraphic sections were selected for dating the sedimentary successions that include the last three volcanic episodes of a total number of 13. The Middle Jurassic volcanic episodes were named V_{11}, V_{12}, and V_{13}, following the logical sequencing already established for the previous ten Lower Jurassic volcanic phases (V_1 to V_{10}, in Cortés 2020a). Nine of the sixteen stratigraphic sections are located in the Caudiel Fault Zone, three in the Alcublas Fault Zone, and four in the Teruel Fault Zone. The ubication of the stratigraphic sections is indicated in Fig. 1A and the geographic coordinates at their midpoint in Tab. 1. All the specimens figured in the stratigraphic sections are stored at the Museo Aragonés de Paleontología, Dinópolis Foundation, Teruel.

The PV.4-9, PV.4-3, CAM.1-2, CAM.1-5, PI-BA.3-1, and PI-BA.2-4 stratigraphic sections, illustrated in Fig. 3, contain information about the stratigraphic position and age of the oldest Middle Jurassic volcanic episode (V_{11}). The volcanic episode V_{12} is included in the CA-1, CA-31, and CA-35 sections (Fig. 4), the PI-BA.1-5 and PI-BA.1-7 sections (Fig. 5), the SA.1-1 and SA.2-1 sections (Fig. 6), as well as in the PI-BA.2-4 stratigraphic section in Fig. 3. The LLÍR-5 (Fig. 7) and the AB-2 and AB-3 (Fig. 8) sections involve the youngest Middle Jurassic volcanic episode (V_{13}).

Lithofacies and sedimentary processes in lithostratigraphic units hosting volcanic rocks

The El Pedregal Formation (lower-middle part) is the Middle Jurassic lithostratigraphic unit that contains the three volcanic deposits, the oldest of them (V_{11}) resting directly on the top of the underlying Casinos Formation. Both formations were defined by Gómez et al. (2003) and Gómez & Fernández-López (2004) across the external Castilian and Aragonese platforms of the Iberian Range.

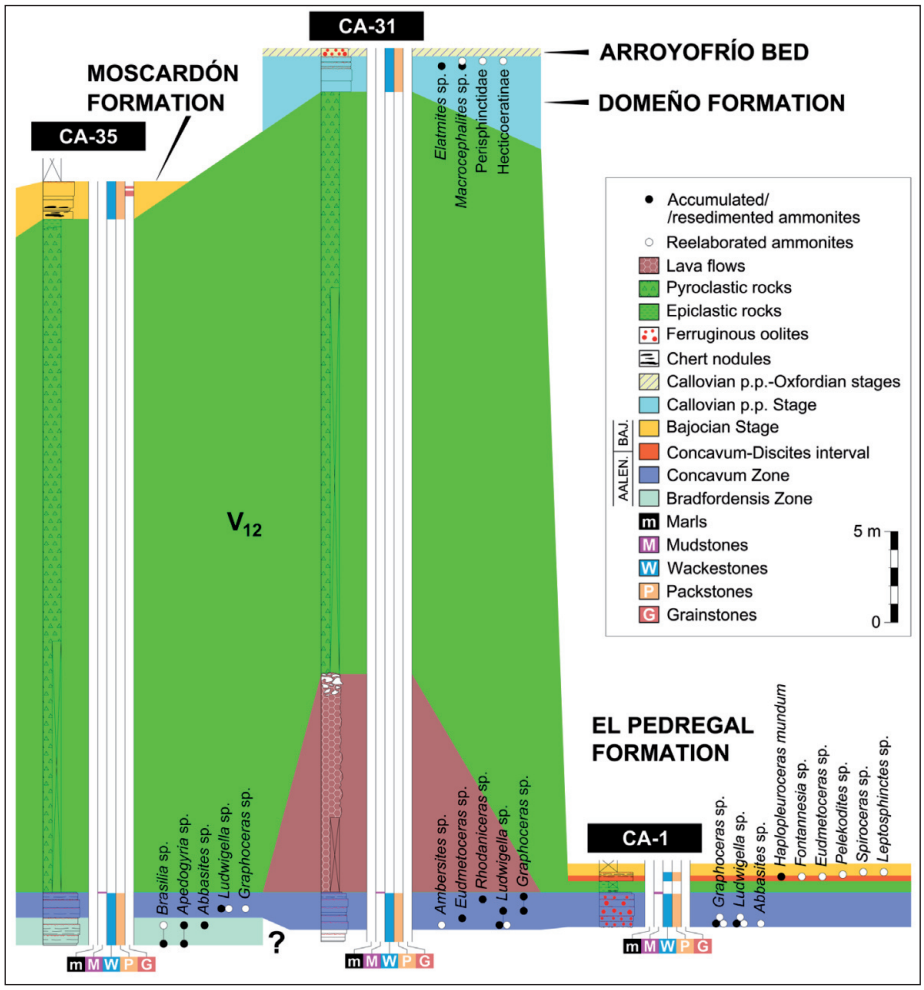

Fig. 4 - CA-1, CA-31, and CA-35 logs (Caudiel Fault Zone) showing the volcanic episode V_{12} interbedded in the lower part of the El Pedregal Formation. The volcanic deposits acquired a mound morphology. Once cemented, the flanks and summit are gradually covered by onlapping lithostratigraphic units (see also Cortés 2020b for a more comprehensive reconstruction of the stratigraphic architecture and the volcanic, tectonic, and sedimentary relationships).

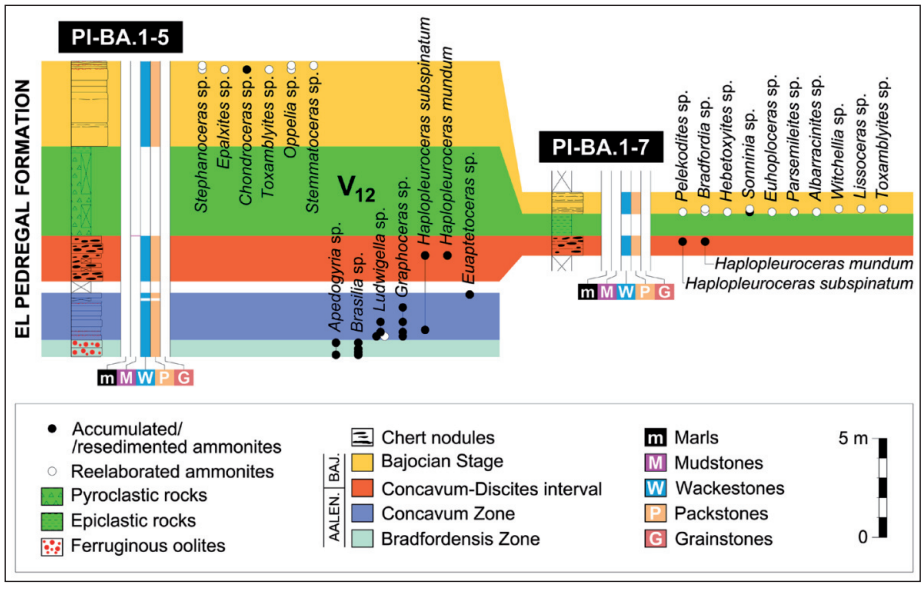

Fig. 5 - PI-BA.1-5 and PI-BA.1-7 logs (Caudiel Fault Zone) showing the volcanic episode V_{12} interbedded in the lower part of the El Pedregal Formation.

The uppermost part of the Casinos Formation was deposited during the early Aalenian. It comprises thin-to-medium-bedded bluish-gray mudstones, reddish-brown or reddish-yellow bioclastic wackestones, and, locally, packstones or even grainstones, with echinoderms (mainly crinoids), bivalves (mainly inoceramids and oysters), gastropods, brachiopods, belemnites, and ammonites, sometimes bearing ferruginous ooids (Fig. $9A_1$, $9A_2$). The beds are commonly arranged into decimetric-to-metric

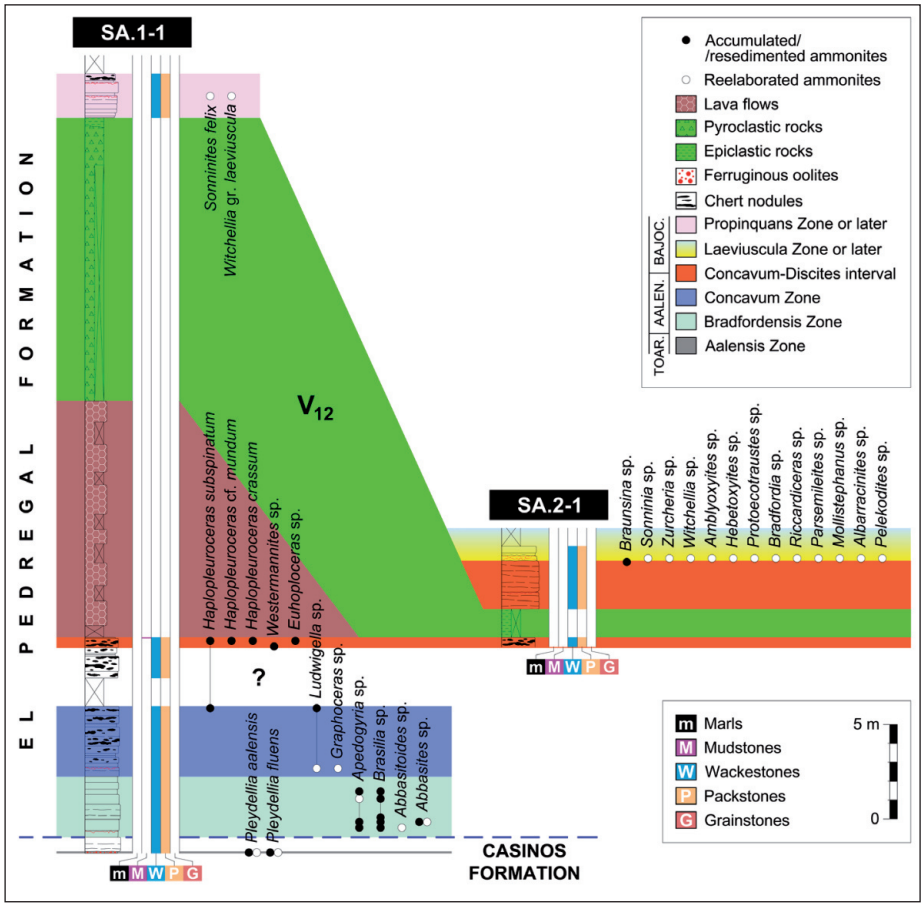

Fig. 6 - SA.1-1 and SA.2-1 logs (Caudiel Fault Zone) showing the volcanic episode V_{12} interbedded in the lower part of the El Pedregal Formation.

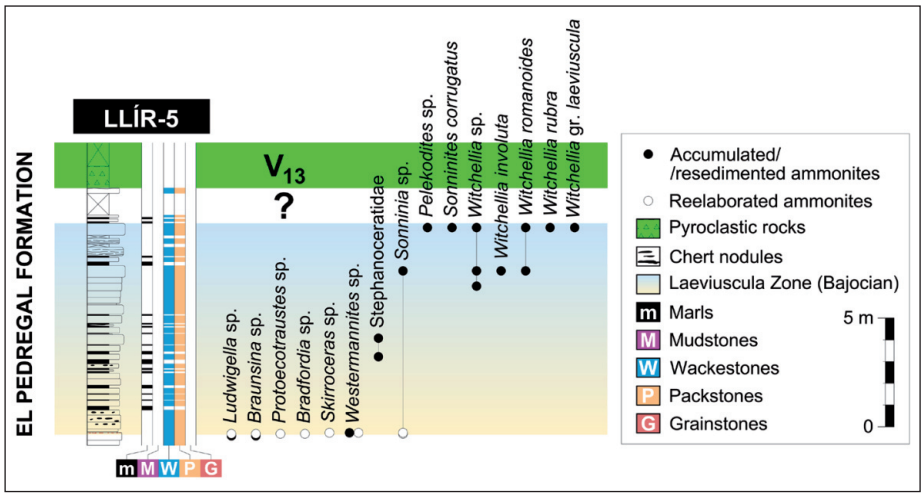

Fig. 7 - LLÍR-5 log (Alcublas Fault Zone) showing the volcanic episode V_{13} interbedded in the lower-middle part of the El Pedregal Formation.

shallowing-, thickening-, and coarsening-upward sequences, which are topped with endured substrates (Fig. $9A_3$).

The lower and middle parts of the El Pedregal Formation were accumulated during the late Aalenian and the early Bajocian. They consist of thinly to thickly bedded bluish-gray mudstones and grayish bioclastic wackestones to packstones (with crinoids, gastropods, bivalves, brachiopods, belemnites, ammonites, and sponges) in which the formation of chert nodules is a distinctive feature. Ferruginous and phosphatic ooids are frequent in the lower Aalenian beds, whereas marl-limestone alternations are often observed in the Bajocian strata (Fig. $9B_1$, $9B_2$, $9C_1$, $9C_2$). The lithologies are generally organized into coarsening-, thickening-, and shallowing-upward sequences (asymmetric cycles), with an occasional thin lower part of marly-limestones and a middle-upper part of limestones capped by bioturbated (mainly *Thalassinoides* trace

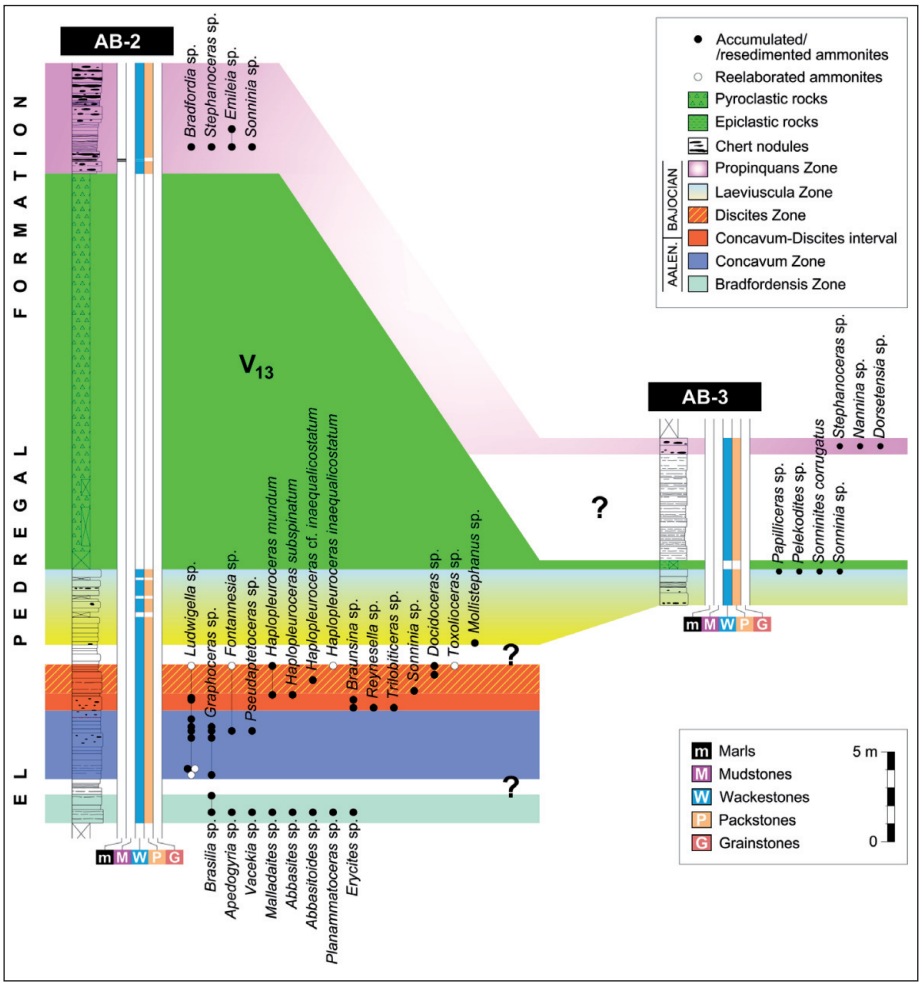

Fig. 8 - AB-2 and AB-3 logs (Alcublas Fault Zone) showing the volcanic episode V_{13} interbedded in the lower-middle part of the El Pedregal Formation.

fossils), Fe-encrusted, and early cemented surfaces (hardgrounds) (Gómez & Fernández-López 2004, 2006) (Fig. $9B_3$, $9C_3$), and also into deepening- and fining-upward sequences (Cortés 2018) as a part of symmetric cycles (Fig. $9C_4$).

Shallowing-upward sequences that developed in the uppermost part of the Casinos Formation (Fig. $9A_3$) can be seen in the PV.4-9, CAM.1-2, CAM.1-5, and PI-BA.2-4 logs in Fig. 3. Shallowing-upward sequences involving the lower part of the El Pedregal Formation (Fig. $9B_3$) are displayed in the PI-BA.2-4 (Fig. 3), CA-1 (Fig. 4), and PI-BA.1-5 (Fig. 5) logs. Asymmetric sequences with a shallowing-upward trend from the lower part of the El Pedregal Formation (Fig. $9C_3$) are included in the CA-31 and CA-35 logs (Fig. 4), in the PI-BA.1-5 and PI-BA.1-7 logs (Fig. 5), in the SA.1-1 log (Fig. 6), in the LLÍR-5 log (Fig. 7), as well as in the AB-2 and AB-3 logs (Fig. 8). Finally, symmetric cycles with deepening- and shallowing-upward trends belonging to the lower-middle part of the El Pedregal Formation (Fig. $9C_4$) are represented in the LLÍR-5 log (Fig. 7).

The sedimentary environments of both formations correspond to a system of external, shallow, open, and fault-controlled carbonate platforms with pelagic fauna and seawater of normal salinity. The sediments were deposited below the fair-weather wave base, but above the storm-wave base (Gómez et al. 2003, 2004; Gómez & Fernández-López 2006). A regionally extensive gap in the stratigraphic record occurred during the Aalenian Murchisonae Zone (Fernández-López 1997; Fernández-López & Gómez 2004; Gómez & Fernández-López 2004, 2006; Gómez et al. 2004), separating the Casinos and the El Pedregal formations.

A gradual shallowing interval, including condensed sections with a low sedimentation rate, a thickness reduction of the stratigraphic intervals, hardgrounds, and gaps in deposition between stratigraphic levels in the upper part of the Casinos Formation, developed during the late Toarcian and culminated with the intra-Murchisonae discontinuity. The platform system experienced a long-term progressive deepening, also with condensed sections

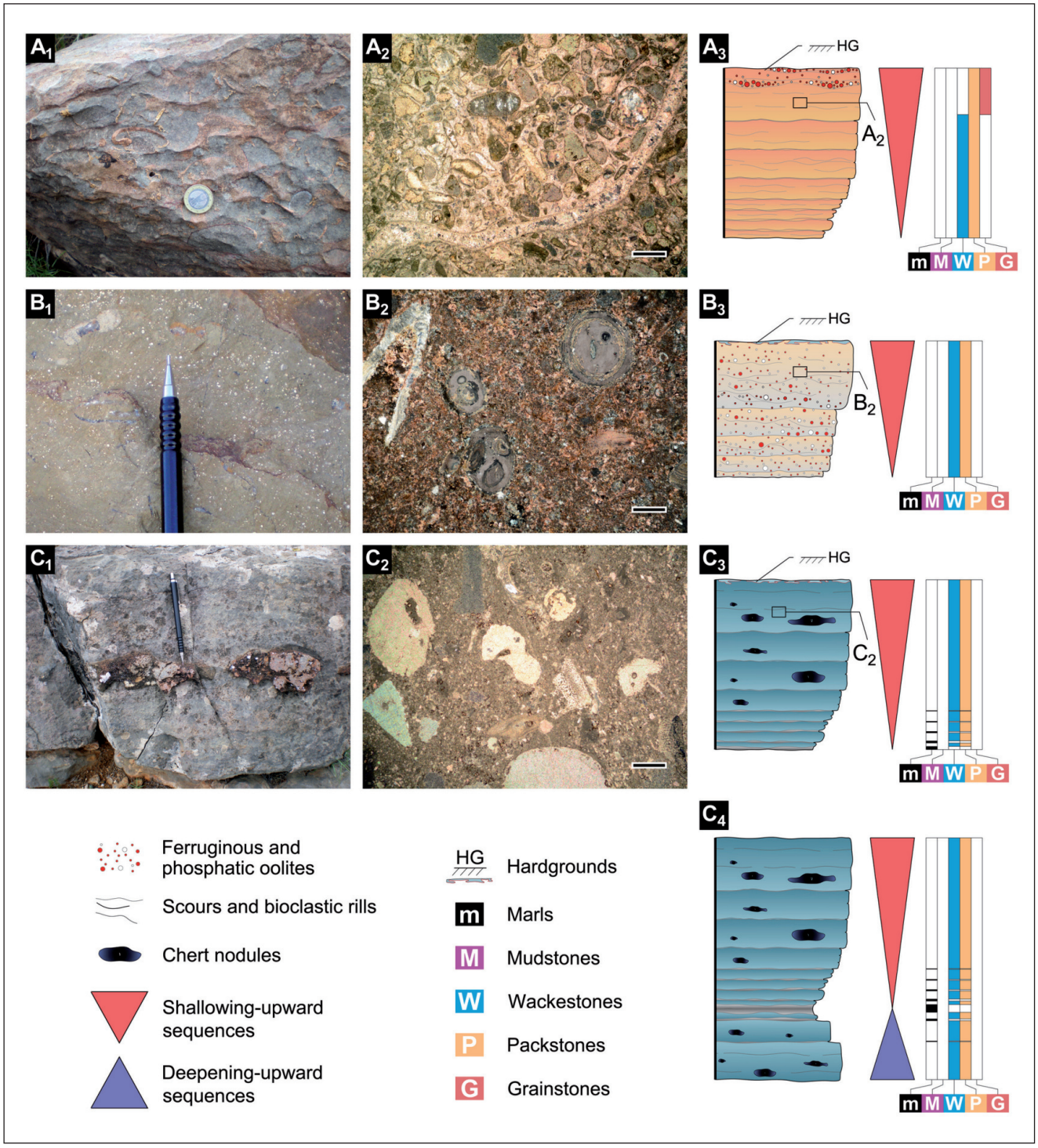

Fig. 9 - Carbonate cycles and main sedimentary lithologies. A_1) Field appearance of the Casinos Formation. A_2) Microfeatures derived from the rock previously photographed (bioclastic grainstones in which the allochems are closely packed and intergranular porosity cemented with equal size spar crystals). A_3) Asymmetric cycle (shallowing-upward arrangements) observed in the Casinos Formation. B_1) Field appearance of the lower part of the El Pedregal Formation. B_2) Thin-section photograph derived from the rock previously photographed (bioclastic and oolitic wackestones to packstones with recrystallization of micrite to microspar mainly affecting the matrix). B_3) Asymmetric cycle (shallowing-upward arrangements) observed in the lower part of the El Pedregal Formation. C_1) Field appearance of the lower-middle part of the El Pedregal Formation. C_2) Microphotograph derived from the rock previously photographed (bioclastic and intraclastic wackestones). C_3) Asymmetric cycle (shallowing-upward arrangements) observed in the lower-middle part of the El Pedregal Formation. C_4) Symmetric cycle (deepening- and shallowing-upward arrangements) observed in the lower-middle part of the El Pedregal Formation. The microfeatures observed under the microscope with cross-polarized light were obtained from the upper portion of the sequences. The scale in A_1) is a 1-euro coin. The pencil used as scale in B_1) and C_1) is 14 cm long. Scale bars in A_2), B_2), and C_2) correspond to 500 μm.

throughout the late Aalenian and earliest Bajocian, from the discontinuity (Murchisonae) to the middle part of the Humphriesianum Zone, followed by a change to a shallowing trend until the end of this same Humprhiesianum Zone (Gómez & Fernández-López 1994; Gómez et al. 2004) (Fig. 2).

Paleodepth conditions from shallow to very moderate water depths, where sediments are occasionally or frequently affected by currents and waves probably induced by storms, may lead to the reworking of unconsolidated sediments and the exhumation of fossil remains. The general absence of hummocky/swaley cross-stratification and of well-developed large-scale cross-bedding in the studied lithostratigraphic units (upper part of the Casinos and lower-middle part of the El Pedregal formations) suggests no high-energy intertidal settings. However, sedimentary structures, such as rills, cut and fill, or scoured surfaces within individual beds (sometimes filled with ferruginous or phosphatic ooids), as well as the concentration of bioclasts, including brachiopods and ammonites, are consistent with storm-induced currents across open platform settings and indicate sedimentation above the storm-influence base. The presence of reelaborated ammonites, along with the sedimentary structures, demonstrates a moderate to high degree of hydrodynamic energy in the sedimentary environment. However, reelaborated and resedimented ammonites are frequently mixed in the same bed or fossiliferous horizon. The conditions needed for the coexistence of reelaborated (previously buried and then exhumed) and resedimented (displaced but neither buried nor exhumed) ammonites are thought to require either only episodic high-turbulence events or the transport of exhumed elements as bedload towards slightly deeper positions; that is, stormy events followed by periods of calm.

Since the low accommodation enhances the conditions of higher turbulence, the degree of removal of the ammonite associations and, therefore, the increasing amount of reelaborated ammonites must show a direct relationship with the proximity to the boundaries in any order of cyclicity. In shallowing-upward sequences, according to Fernández-López (1997), the higher rate of reelaborated ammonites is evident towards their top, but it occurs at the bottom in deepening-upward ones. The reelaboration of ammonites is strongly perceptible near the boundaries of cycles. The intra-Murchisonae discontinuity constitutes a limit of fifth-, fourth-, third-, second-, and first-order cycles and separates the Casinos from the El Pedregal Formation; therefore, both the uppermost part of the Casinos Formation and the lowermost portion of the El Pedregal Formation are prone to contain a high number of reelaborated ammonites (Fernández-López 1997) (e.g., sequences related to the top of the Casinos Formation in Fig. 3 or the bottom of the El Pedregal Formation in Fig. 4. Also, within the El Pedregal Formation linked this time with the top of fifth-order sequences in Figs. 5 and 6). In summary, the upper part of the Casinos Formation and the lower portion of the El Pedregal Formation show similar features concerning sedimentary processes, but the former displays a general high-rank shallowing-upward trend and the later, by contrast, a general high-rank deepening-upward stacking of lithofacies.

Other lithostratigraphic units related to the volcanics, sometimes directly covering their flanks and tops, are the Moscardón Formation, the Domeño Formation, and the Arroyofrío Bed. This is a peculiar characteristic of the Caudiel outcrop concerning the volcanic episode V_{12} (see CA-1, CA-31, and CA-35 logs in Fig. 4). As a general rule, the Middle Jurassic volcanic levels in the studied region are covered by the El Pedregal Formation strata (Bajocian in age). However, in the Caudiel outcrop (Figs. 1A and 4), significant omissions in sedimentation occurred during the Middle Jurassic (e.g., the Discites and Laeviuscula Bajocian zones, the middle and late Bathonian, as well as, presumably, a relevant part of the Callovian are absent; Fernández-López et al. 1985; Cortés 2018, 2020b), as a result of low subsidence rates or even uplifted and tilted blocks (Cortés 2020b).

The Moscardón Formation, defined by Gómez & Fernández-López (2004), is composed of bioclastic and oolitic packstones to grainstones, with abundant crinoids, ooids and intraclasts. Chert nodules and sedimentary structures such as cross-lamination, bioclastic rills, and bars are frequent. This unit was dominated by open-marine, high-energy, and very shallow environments of normal salinity.

The Domeño Formation was defined by Gómez & Fernández-López (2004). It consists of well-stratified grayish wackestones, packstones, and locally mudstones, bearing mainly microfilaments (thin-shelled bivalves), echinoderms, brachiopods,

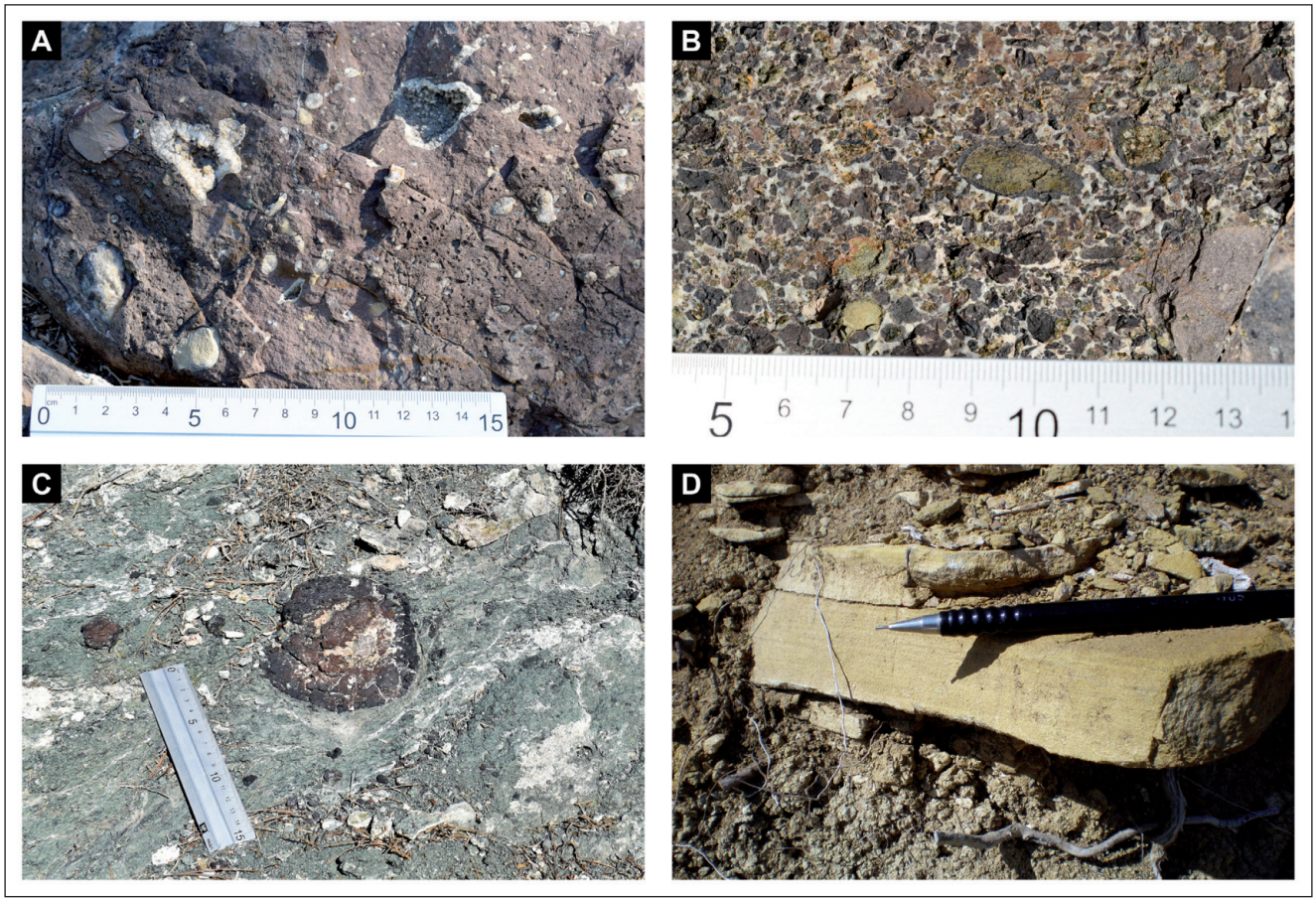

Fig. 10 - Main volcanic lithologies. A) Vesicular lava flow. B) Lapillistones or lapilli. C) Lapilli-tuff deposits including basaltic bombs. D) Epiclastic tuffaceous sandstones. Volcanic rocks from A), B), and C) belong to the volcanic episode V_{12} in the CA-31 section. Volcanosedimentary deposit from C) belongs to the volcanic episode V_{12} in the PI-BA.1-7 section. The ruler used as scale in C) is 16 cm long, and the pencil in D),14 cm.

belemnites, ammonites, chert nodules, and trace fossils (*Thalassinoides* and *Zoophycos*). Calcareous oolitic grainstones can develop in the lower part; however, interbedded marly limestones may also be common. The beds are arranged into thickening- and shallowing-upward sequences showing bioturbated and encrusted surfaces (hardgrounds) at the top.

The Arroyofrío Bed was defined by Gómez & Goy (1979) as successive reddish-gray ferruginous oolitic and pisolitic ironstone levels separated by erosive surfaces. It contains mainly bivalves, brachiopods, echinoderms, belemnites, and ammonites. Ooids are displayed both packed and scattered, often showing accretionary growth around a lithoclastic or bioclastic nucleus.

The sediments of the Domeño Formation (Bathonian-Callovian) were deposited on an open-marine, low-energy, and external carbonate platform of normal salinity. The Arroyofrío Bed (upper Callovian-lower Oxfordian), located at the top of the Domeño Formation, reflects a homogeneous shallowing of the carbonate platforms, reaching even emersion phases with an associated hiatus at a regional scale (Gómez & Fernández-López 2006).

Nature of volcanic rocks

The Middle Jurassic volcanics of the Iberian Range are represented by submarine basaltic rocks with a chemical alkaline affinity (Ancochea et al. 1988). The rock types constituting the volcanic episodes V_{11}, V_{12}, and V_{13} mainly consist of fragmental greenish volcaniclastic deposits and minority massive dark purple to greenish lavas, the latter representing far less than 5% of the total of the volcanic products released.

From a petrographic viewpoint, the volcanic materials (both volcaniclastic and coherent lavas) are olivine-rich basalts and, exceptionally, plagioclase-rich basalts. Lavas show a porphyritic texture with olivine and clinopyroxene phenocrysts dispersed within a clinopyroxene, plagioclase, and olivine finer-grained microlite-rich groundmass. In

volcaniclastic products, vesicular and glassy shards dominate over scarce, either olivine or plagioclase, phenocrysts. They present a very high degree of alteration, dominating silicification and serpentinization processes (Ancochea et al. 1988).

Lavas generally acquire a dome-like shape of small thickness and length showing a high content of vesicles, which are usually infilled with calcite (Fig. 10A) as a result of syn- or post-volcanic hydrothermal processes and pore water circulation (Ancochea et al. 1988; Cortés & Gómez 2016; Cortés 2020a). Regarding the explosive volcanics, two main genetic categories can be distinguished: primary pyroclastic deposits and secondary pyroclastic (volcano-sedimentary or epiclastic) ones (White & Houghton 2006; Sohn & Sohn 2019). In this work, primary pyroclastic accumulations include those that display original textures by eruption and emplacement processes and those resedimented by syneruptive volcaniclastic processes (e.g., primary mass flows and turbidite currents). Pyroclastic accumulations are rich in juvenile lava fragments and accidental lithic clasts, introduced by the inherent explosive processes and derived from the magma and the sedimentary country rocks, respectively. Based on the grain size terms used for primary pyroclastic rocks (Fisher & Schmincke 1984; McPhie et al. 1993), the Middle Jurassic pyroclastic deposits of the studied area can be essentially classified as lapillistones –or lapilli, following the criteria of White & Houghton (2006)– (Fig. 10B), lapilli-tuffs (Fig. 10C), or tuffs, according to the proportion of lapilli and ash particles. The second type of volcaniclastic deposits (that is, the epiclastic or volcano-sedimentary materials) consists of reworked pyroclastic debris constituting fine-grained tuffaceous sandstones (Fig. 10D) and siltstones (see Cortés & Gómez 2016 and Cortés 2020a).

Given that a single clastic volcanic deposit can usually accommodate the complete spectrum of possible primary pyroclastic and secondary epiclastic types, it has been found more functional to use only pyroclastic and epiclastic terms in the figures. Since submarine erosive agents, such as waves or currents, are prone to accumulate epiclastic deposits in distal margins of original volcanic bodies (expanding their limits and eroding their summits), the presence of solely epiclastic deposits is congruent with minor volcanic thicknesses of pinchout areas, as can be seen in the following logs: PI-BA.2-4, PI-BA.3-1, PV.4-3, PV.4-9, and CAM.1-5 (Fig. 3), CA-1 (Fig. 4), PI-BA.1-7 (Fig. 5), SA.2-1 (Fig. 6), and AB-3 (Fig. 8).

Biochronostratigraphic framework

PV.4-3 log (Fig. 3) - The Murchisonae discontinuity marks the contact between the Casinos and El Pedregal formations, underlines the boundary between the second-order LJ-4 and MJ-1 cycles, and implies the establishment of very shallow-water sedimentary conditions, even including, at least, intermittent subaerial exposures (Fernández-López 1997). This means that the immediately previous and subsequent sedimentary successions were deposited under a high degree of turbulence. Rills, scours, oolithic lithologies, or grain-supported textures are frequent in strata located below and above the Murchisonae discontinuity. Likewise, paleontological remains often underwent successive episodes of exhumation and burial (e.g., reelaborated ammonites).

Although the species *Esericeras fascigerum* (i.e., the index of the Fascigerum Subzone, Thouarsense Zone, according to Goy & Martínez 1990 and Page 2003) has not been found, *Esericeras eseri* (w) has also been situated in the Thouarsense Zone (e.g., Neige & Ruget 2002; Rulleau 2010). However, its reelaborated taphonomic state provides a Thouarsense Zone age or younger to the sedimentary bed containing it. The occurrence of brachiopod species belonging to the Assemblage 5, such as *Stroudithyris infraoolithica* (extending from the lower part of the Variabilis Zone to the end of the Dispansum Zone, according to García Joral & Goy 2000), and *Homoeorhynchia*? *marini* (ranging from the base of the Variabilis Zone to the end of the Pseudoradiosa Zone, according to García Joral et al. 2016), together with *Esericeras eseri* (w) would put the Dispansum or Pseudoradiosa zones as the most likely maximum age for the pre-volcanic sediments.

Concerning the post-volcanic sediments, the Aalenian Concavum Zone can be already identified from the first record of *Ludwigella* sp. (w) until probably the last record of *Graphoceras* sp. (r) and *Ludwigella* sp. (r/w). Above, *Reynesella* sp. (w) would almost certainly be indicative of the Bajocian Discites Zone, according to Fernández-López (1985) and García-Frank (2006).

PV.4-9 log (Fig. 3) - Despite the term "cf.", *Pseudogrammoceras* cf. *fallaciosum* (r) would identify

the Thouarsense Zone, according to Page (2003). *Stroudithyris infraoolithica* (lower part of the Variabilis Zone-end of the Dispansum Zone, according to García Joral & Goy 2000), present in the same fossiliferous level, is consistent with this determination.

Above, the taphonomic state of *Pseudolillia murvillensis* (w) could be representative of the Dispansum Zone (Goy & Martínez 1990) or younger.

Pleydellia cf. *mactra* (w) and *Pleydellia* cf. *aalensis* (w), which occur underneath the volcanic deposit in the upper part of the Casinos Formation, are indicative of the Aalensis Zone (according to Goy & Martínez 1990 and Page 2003). However, once again, the reelaborated state could characterize the Aalensis or any younger zone below the volcanic base. Nevertheless, the temporal distribution of the brachiopod specimens belonging to the Assemblage 6 (Pseudoradiosa-Aalensis, according to Baeza-Carratalá et al. 2016), such as *Stroudithyris stephanoides* and *Rynchonelloidea* cf. *goyi*, is compatible with the Aalensis Zone.

In the post-volcanic El Pedregal Formation, the Aalenian Concavum Zone is identified with certainty by the first occurrence of *Ludwigella* sp. (r), and the content of the last fossiliferous level (resedimented specimens of *Haplopleuroceras* sp. and *Toxolioceras* sp.) could indicate the Bajocian Discites Zone (according to Fernández-López 1985 and García-Frank 2006).

CAM.1-2 log (Fig. 3) - According to the Toarcian biozonation by Goy & Martínez (1990), *Podagrosites* cf. *aratum* (r) and *Pseudogrammoceras* cf. *subregale* (r) identify the upper part of the Toarcian Variabilis Zone (probably the Illustris Subzone), whereas *Pseudogrammoceras* cf. *muelleri* (r) may indicate either the upper part of the Variabilis Zone or the lower part of the *Thouarsense* Zone.

On the one hand, *Pseudogrammoceras* cf. *fallaciosum* (w), occurring 4.55 m above, is a time marker for the Fallaciosum Subzone (upper part of the Thouarsense Zone). On the other hand, *Pseudolillia* sp. (w) identifies the Dispansum Zone. The reelaborated taphonomic state of both species confers a Thouarsense or Dispansum Zone age or younger, respectively, to the beds containing them.

In the 0.60 m thick post-volcanic bed, belonging to the El Pedregal Formation, no ammonites have been found.

CAM.1-5 log (Fig. 3) - *Pseudogrammoceras* cf. *fallaciosum* (r) points to a Fallaciosum Subzone (Thouarsense Zone) age for the bed in which it is included; and *Pseudolillia* sp. (w), above it, marks a Dispansum Zone age or younger (according to Goy & Martínez 1990) for the sediments positioned below and the closest to the volcanic base. The Graphoceratidae (r) and Hammatoceratidae (r) specimens in the post-volcanic sediments probably identify the Aalenian Concavum Zone.

PI-BA.3-1 log (Fig. 3) - The ammonite assemblage from the upper part of the Casinos Formation contains species that lived at different times (at least, both the Toarcian Aalensis Zone and the Aalenian Opalinum Zone are represented, according to Ureta et al. 1999, Sandoval et al. 2001, and García-Frank 2006), and were finally mixed (under high-energy conditions), buried, and fossilized together. Since all of them show a reelaborated taphonomic state, the bed located immediately below the volcanic deposit from which they were extracted could be Aalenian Opalinum Zone or younger in age.

PI-BA.2-4 log (Fig. 3) - The ammonite assemblage from the pre-volcanic interval (Casinos Formation) includes representative species of the Toarcian Aalensis Zone, the Aalenian Opalinum Zone [e.g., *Leioceras crassicostatum* (w), found about 0.50 m from the top of the Casinos Formation (Fig. 11A)], and the Aalenian Murchisonae Zone [e.g., *Spinammatoceras tenax* (w), found about 0.50 m from the top of the Casinos Formation (Fig. 11B), or *Ancolioceras opalinoides* (w), found 0.30 m from the top of the formation (Fig. 11C)], according to Ureta et al. (1999), Sandoval et al. (2001), and García-Frank (2006). All the specimens are reelaborated elements (as a result of a high degree of water turbulence), so they allow assigning a Murchisonae age or younger to the upper limit of the Casinos Formation. However, as stated by Gómez et al. (2003), the top of the Casinos Formation in the Iberian Range matches a basin-wide discontinuity which is located within the Murchisonae Zone, the so-called intra-Murchisonae discontinuity issued in Fernández-López (1997), Fernández-López & Gómez (2004), Gómez & Fernández-López (2004, 2006), and Gómez et al. (2004). Therefore, the Murchisonae Zone is the upper age limit that can reach the top of the Casinos Formation in the PI-BA.2-4 section.

On the basis of the works by Fernández-López (1985) and García-Frank (2006), the appearance of *Ludwigella* sp. (r) (Fig. 11D) in the lower

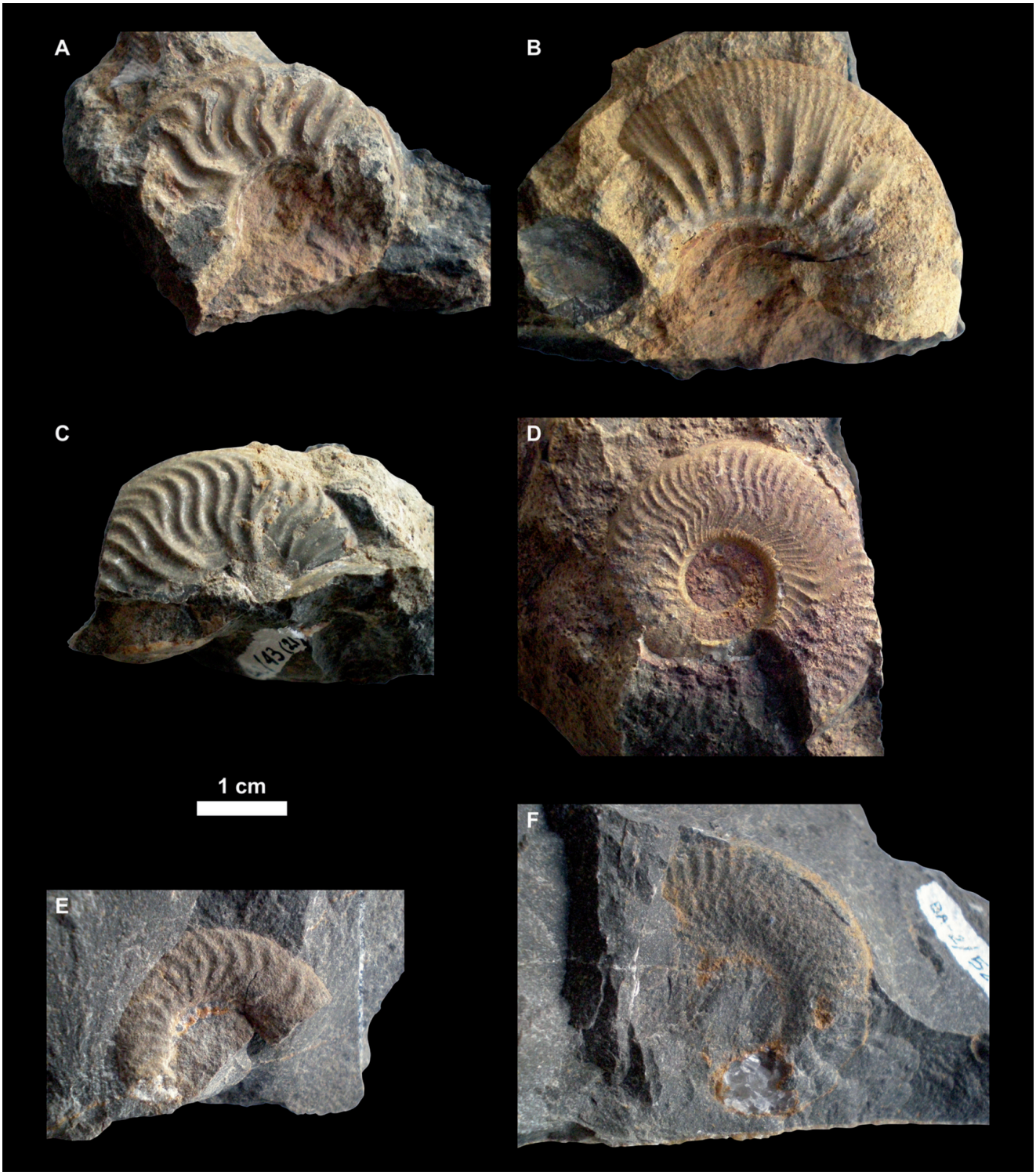

Fig. 11 - Representative ammonite species from the upper part of the Casinos Formation and the lower part of the El Pedregal Formation in the PI-BA.2-4 stratigraphic section. A) *Leioceras crassicostatum* (w); B) *Spinammatoceras tenax* (w); C) *Ancolioceras opalinoides* (w); D) *Ludwigella* sp. (r); E) *Reynesella* sp. (r); F) *Braunsina* sp. (r).

part of the pre-volcanic El Pedregal Formation (ferruginous oolitic beds) allows the recognition of the Aalenian Concavum Zone. This zone would extend until the uppermost 0.40m of the log where *Graphoceras* sp. (r), *Haplopleuroceras* sp. (r), *Reynesella* sp. (r) (Fig. 11E), and *Braunsina* sp. (r) (Fig. 11F) may indicate either the latest Aalenian Concavum Zone or the earliest Bajocian Discites Zone.

CA.1 log (Fig. 4) - Resedimented and reelaborated elements of *Graphoceras* sp. and *Ludwigella* sp.

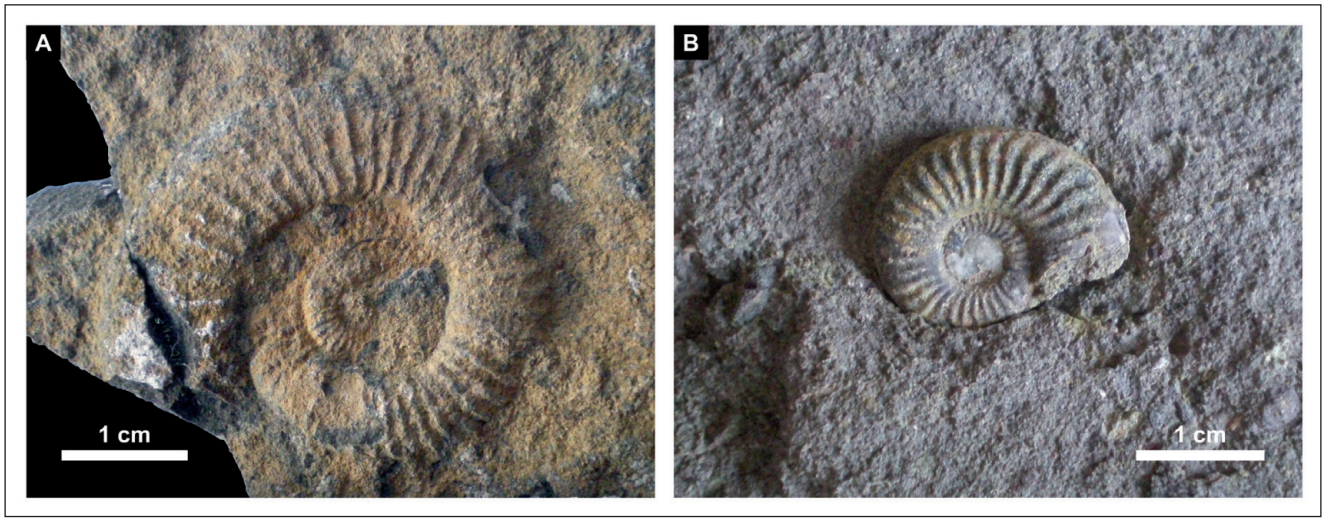

Fig. 12 - Ammonite species from the lower part of the El Pedregal Formation in the PI-BA.1-7 and near the SA.2-1 sections. A) *Haplopleuroceras mundum* (r) obtained in the sediments located below the volcanic episode V_{12} in the PI-BA.1-7 section; B) Internal mold of *Fontannesia grammoceroides* (r) found within the volcaniclastic deposit (volcanic level V_{12}) near the SA.2-1 section. There is neither difference, nor presence of structural discontinuity, between the composition of the mold infilling and the enclosing volcaniclastics. In addition, traces of disarticulation, fracture, abrasion, bioerosion, or encrusting organisms are non-existent. The most inner whorls show incomplete infilling, remaining hollow, to be cemented later with macrocrystalline calcite.

have been found in the lower part of the log. These specimens consistently characterize the Aalenian Concavum Zone (according to Fernández-López 1985 and García-Frank 2006).

The ammonite assemblage, located 0.25 m above the volcanics [*Haplopleuroceas mundum* (r), *Fontannesia* sp. (w), and *Eudmetoceras* sp. (w)], does not clearly identify the Aalenian Concavum Zone nor the Bajocian Discites Zone, given that these species are representative of both zones.

The upper part of the interval contains *Pelekodites* sp. (w) (Bajocian Laeviuscula Zone-Bajocian Humphriesianum Zone, according to Fernández-López 1985). Above, *Leptosphinctes* sp. (w) and *Spiroceras* sp. (w) characterize the late Bajocian, according to Fernández-López (1985).

CA-31 log (Fig. 4) - The Aalenian Concavum Zone has been identified by resedimented specimens of *Graphoceras* sp. and *Ludwigella* sp., according to Fernández-López (1985) and García-Frank (2006), in pre-volcanic sediments. Above the volcanics, the Callovian Stage could be characterized by *Macrocephalites* specimens.

CA.35 log (Fig. 4) - The Aalenian Bradfordensis Zone is recognized by the occurrence of *Brasilia* sp. (r) and *Apedogyria* sp. (r) (Fernández-López 1985 and García-Frank 2006). The Aalenian Concavum Zone has been identified by resedimented specimens of *Ludwigella* sp., according to Fernández-López (1985) and García-Frank (2006).

PI-BA.1-5 log (Fig. 5) - The Aalenian Bradfordensis Zone is recognized by the occurrence of *Brasilia* sp. (r) and *Apedogyria* sp. (r) (Fernández-López 1985 and García-Frank 2006) in the lower oolitic beds. The Aalenian Concavum Zone has been identified by resedimented specimens of *Graphoceras* sp. and *Ludwigella* sp., according to Fernández-López (1985) and García-Frank (2006). Above, the fossil content (resedimented specimens of *Haplopleuroceras subspinatum* and *Haplopleuroceras mundum*) may indicate the upper part of the Concavum Zone (Aalenian), as well as the lower part of the Discites Zone (Bajocian), according to Fernández-López (1985) and García-Frank (2006).

The early Bajocian is identified by the occurrence of the post-volcanic ammonite associations.

PI-BA.1-7 log (Fig. 5) - The fossil content of the pre-volcanic sediments [*Haplopleuroceras subspinatum* (r) and *Haplopleuroceras mundum* (r) (Fig. 12A)] may indicate the upper part of the Concavum Zone (Aalenian), as well as the lower part of the Discites Zone (Bajocian), according to Fernández-López (1985) and García-Frank (2006). The post-volcanic ammonite associations characterize the early Bajocian.

SA.1-1 log (Fig. 6) - The Toarcian Aalensis Zone is characterized by the specimens of *Pleydellia* in the pre-volcanic Casinos Formation (according to Goy & Martínez 1990). The Aale-

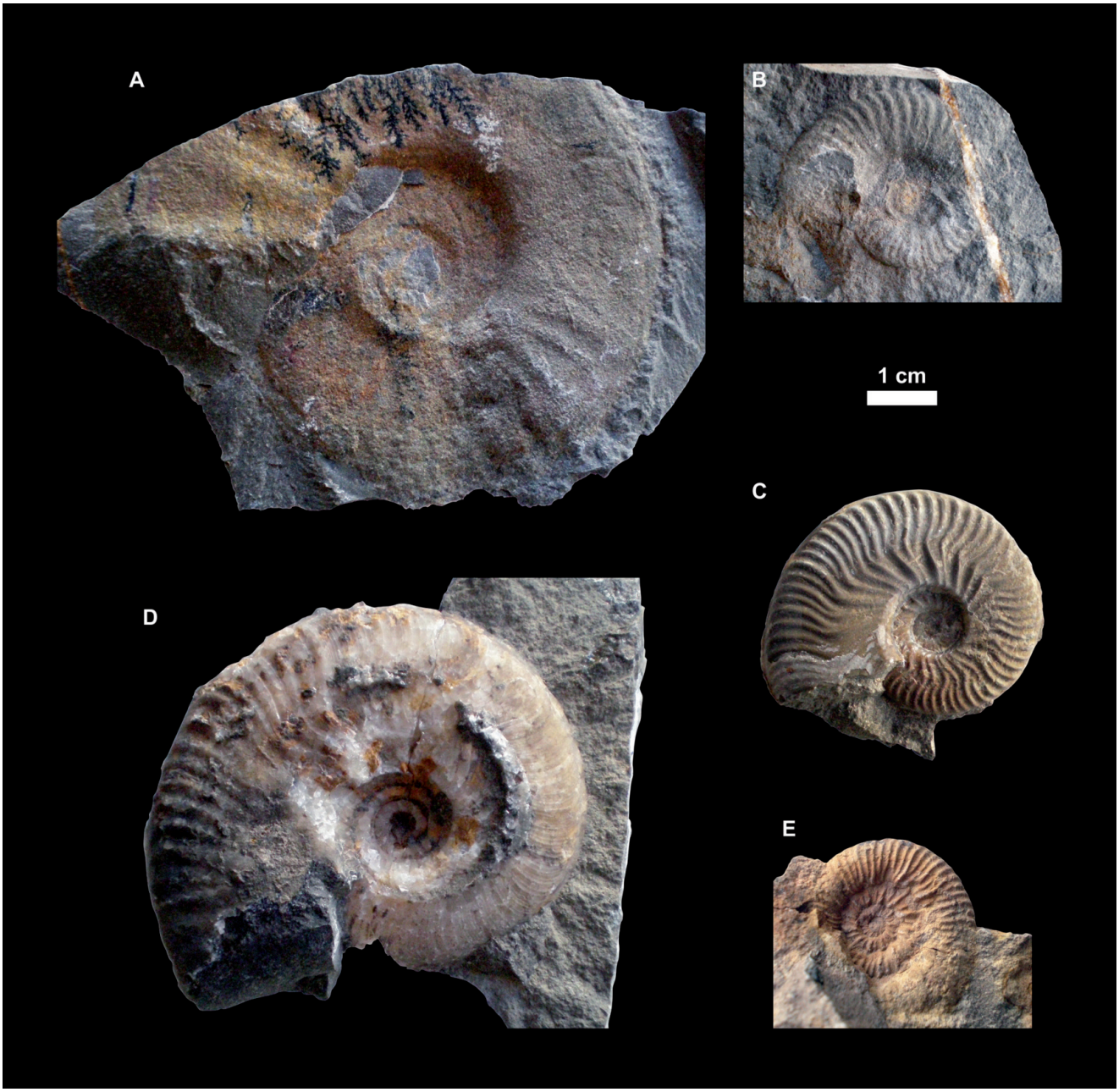

Fig. 13 - Ammonite species from the lower-middle part of the El Pedregal Formation, below the volcanic level V_{13} in LLÍR-5 and AB-2 sections. A) *Witchellia romanoides* (r); B) *Sonninites corrugatus* (r); C) *Apedogyria* sp. (r); D) *Brasilia* sp. (r); E) *Haplopleuroceras inaequalicostatum*. (w). Specimens A) and B) have been found in the LLÍR-5 section. Specimens C), D), and E) in the AB-2 section.

nian Bradfordensis Zone is recognized by the occurrence of *Brasilia* sp. (r) and *Apedogyria* sp. (r) (Fernández-López 1985 and García-Frank 2006). Resedimented specimens of *Ludwigella* sp. identify the Aalenian Concavum Zone, according to Fernández-López (1985) and García-Frank (2006). The fossil content of the uppermost pre-volcanic 0.50 m may indicate the upper part of the Concavum Zone (Aalenian), as well as the lower part of the Discites Zone (Bajocian), according to Fernández-López (1985) and García-Frank (2006).

The post-volcanic sediments (El Pedregal Formation) belong to the Bajocian Propinquans Zone or younger in age, based on the occurrences of reelaborated specimens of *Sonninites felix* (according to Fernández-López 1985).

SA.2-1 log (Fig. 6) - The ammonite assemblage from the post-volcanic beds shows taphonomic condensation, evidenced by a mixture of reelaborated elements representing different chronostratigraphic units. In this case, the low accommodation that enhances fossiliferous reelaboration and

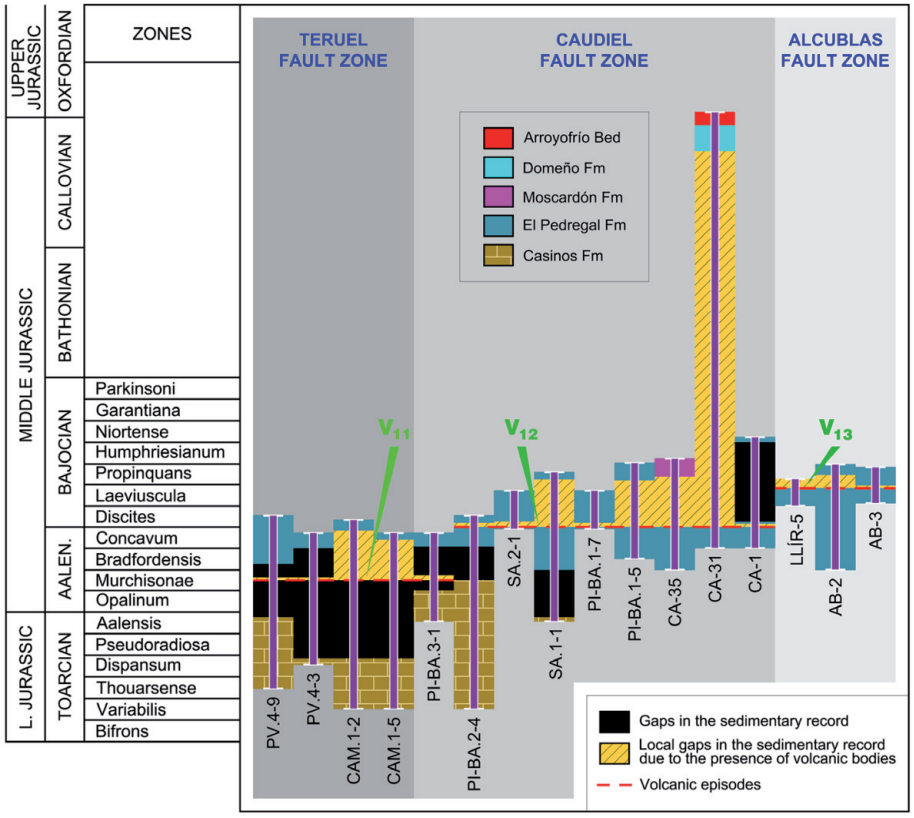

Fig. 14 - Chronostratigraphic extent of the stratigraphic sections and temporal distribution of volcanic episodes along the Teruel, Caudiel, and Alcublas fault zones.

condensation is related to a minor cycle boundary (fourth or fifth order). Based on the stratigraphic distribution of ammonite Bajocian taxa stated by Fernández-López (1985), the fossil assemblage could be indicative of an age corresponding to the Laeviuscula-Propinquans interval. Below this ammonite assemblage, the only specimen of *Braunsina* sp. (r) does not resolve whether the bed containing it is Aalenian (Concavum Zone) or Bajocian (Discites Zone) in age.

LLÍR-5 log (Fig. 7) - According to Fernández-López (1985), the ammonite assemblage of the first fossiliferous level (resedimented specimens of *Ludwigella* sp. and *Braunsina* sp.) characterizes the Aalenian Concavum Zone or the Bajocian Discites Zone, and the reelaborated specimens of *Skirroceras* sp. (w) identify, at least, the Bajocian Laeviuscula Zone in the third fossiliferous level, this zone also being indicated by the ammonite assemblage of the last fossiliferous level [e.g., *Witchellia romanoides* (r) (Fig. 13A) or *Sonninites corrugatus* (r) (Fig. 13B)].

AB-2 log (Fig. 8) - According to Fernández-López (1985), the ammonite assemblage of the first and second fossiliferous levels characterizes the Aalenian Bradfordensis Zone [e.g., *Apedogyria* sp (r) (Fig. 13C) or *Brasilia* sp. (r) (Fig. 13D)]. The Aalenian Concavum Zone is detected from the third to the eighth fossiliferous levels. A Concavum-Discites interval would be extended from the ninth to the twelfth fossiliferous levels (reddish-orange color in the figure). Above, *Sonninia* sp. (r), along with *Toxolioceras* sp. (w) or *Haplopleuroceras inaequalicostatum* (w) (Fig. 13F), indicates the presence of the Bajocian Discites Zone. Probably, *Mollistephanus* sp. (r) in the last fossiliferous level already identifies the Bajocian Laeviuscula Zone.

AB-3 log (Fig. 8) - According to Fernández-López (1985), the ammonite assemblage from the pre-volcanic sediments indicates at least the presence of the Bajocian Laeviuscula Zone, although it could also be representative of the Bajocian Propinquans Zone. The post-volcanic fossiliferous level may characterize both the Laeviuscula and the Propinquans Zone.

Discussion

Spatio-temporal distribution of volcanic deposits

Interbedded within the Middle Jurassic sedimentary successions of the studied area, three volcanic episodes of different ages have been distinguished. From oldest to youngest, they are called

V_{11}, V_{12}, and V_{13}, following the ten Lower Jurassic volcanic phases (V_1 to V_{10} in Cortés 2020a). Fig. 14 shows the temporal distribution of volcanic episodes disposed along the Teruel, Caudiel, and Alcublas fault zones.

Volcanic episode V_{11}. This episode is entirely volcaniclastic with no lava flows, in which pyroclastic and epiclastic terms can be detected. V_{11} crops out in two separate geographic areas: the northwestern outcrops (PV.4-3, PV.4-9, CAM.1-2, and CAM.1-5 stratigraphic sections along the Teruel Fault Zone), and the southeastern outcrops (PI-BA.2-4, PI-BA.3-1 stratigraphic sections along the Caudiel Fault Zone) (Fig. 1A). In both regions, V_{11} is located at the bottom of the El Pedregal Formation overlying the top of the Casinos Formation.

The accurate biochronostratigraphic control reflects how the top of the Casinos Formation may end up being highly diachronous from the northwestern to the southeastern outcrops (Fig. 3). The youngest chronostratigraphic zone recognized for the uppermost part of the Casinos Formation in the NW outcrops is the Toarcian Aalensis Zone (PV.4-9 section), the Dispansum Zone being the most commonly identified (CAM.1-2, CAM.1-5, and, possibly, PV.4-3 sections). By contrast, a significantly more modern Aalenian Opalinum or Murchisonae Zone has been detected in the SE outcrops (PI-BA.3-1 and PI-BA.2-4 sections), consistent with the maximum age estimated by Gómez et al. (2003) for the top of the Casinos Formation across the Iberian Range.

The almost identical ammonite assemblage recorded directly below the base of the volcanic body both in PI-BA.3-1 and PI-BA.2-4 sections (the latter without volcanic deposits) demonstrates that the volcanic deposit lies on the top of the Casinos Formation, and it can supersede the basal part of the El Pedregal Formation, with no apparent replacement in the uppermost part of the Casinos Formation. Besides, thin, or even non-existent, volcanic thicknesses can be observed in several stratigraphic sections of both geographic sectors (e.g., PV.4-3 and PV.4-9 in the NW area, or PI-BA.2-4 in the SE), in which significant regional variations in age for the uppermost sediments of the pre-volcanic Casinos Formation have been revealed. All these data suggest that the greater volcanic thicknesses (e.g., CAM.1-2, CAM.1-5, or PI-BA.3-1 sections) are not responsible for this diachroneity, as no significant portion of the Casinos Formation is being replaced by them. Instead, a tectonically driven origin better explains the pre-volcanic stratigraphic gaps, whose length of time would vary from one outcrop to another. The longer duration of the hiatus along northwestern outcrops results in the time amplification of the intra-Murchisonae discontinuity. Taking into account that time-marker specimens from the Murchisonae Zone are present in pre-volcanic sediments along the southeastern outcrops, the base of the volcanic deposits has been theoretically considered as a more isochronous surface than the top of the Casinos Formation. Therefore, the volcanic deposits located between the Casinos and El Pedregal formations should be regarded as the same volcanic episode V_{11} in all the locations where they crop out, and its age should be estimated as Aalenian Murchisonae Zone (most probably post-Murchisonae discontinuity).

Volcanic episode V_{12}. This episode is hosted in the lower part of the El Pedregal Formation, and it remains virtually confined to the Caudiel Fault Zone (CA-1, CA-31, CA-35, PI-BA.1-5, PI-BA.1-7, PI-BA.2-4, SA.1-1, and SA.2-1 stratigraphic sections, Fig. 1A). V_{12} is volcaniclastic in composition on most sites where it crops out, except in the CA-31 (Fig. 4) and SA.1-1 (Fig. 6) sections, where lava flows of small areal extension and thickness can be observed. Locally, ball-shaped lava bodies, centimetric to decimetric in diameter, are included within thick masses of volcaniclastic accumulations near the SA.2-1 section.

In the CA-1, CA-31 and CA-35 sections (Fig. 4), as well as in the PI-BA.2-4 section (Fig. 3), resedimented and reelaborated elements of *Graphoceras* sp. and *Ludwigella* sp. have been found in sediments located immediately below the volcanics. These specimens consistently characterize the Aalenian Concavum Zone (according to Fernández-López 1985 and García-Frank 2006).

Both in the PI-BA.1-5 and PI-BA.1-7 sections (Fig. 5), the sediments placed just below the volcanic base have not yielded any specimen of the family Graphoceratidae, but they contain *Haplopleuroceras subspinatum* (r) and *H. mundum* (r). These fossils may indicate the upper part of the Concavum Zone (Aalenian), as well as the lower part of the Discites Zone (Bajocian), according to Fernández-López (1985) and García-Frank (2006).

Just like in the case of the PI-BA.1-5 and PI-BA.1-7 sections, in the SA.1-1 (Fig. 6), the ammonite assemblage located immediately below the volcanic base [*Haplopleuroceras subspinatum* (r), *H.* cf. *mundum* (r), *H. crassum* (r), *Westermannites* sp. (r), and *Euhoploceras* sp. (r)] does not allow a differentiation between the Concavun (Aalenian) and the Discites (Bajocian) zones. However, the apparent lack of the first occurrences of the forms accepted as an irrefutable proof to detect the Bajocian Discites Zone, such as the genus *Hyperlioceras* (Fernández-López 1985; García-Frank 2006) or the *Hyperlioceras-Toxolioceras* group (Fernández-López et al. 1988; Henriques et al. 1996; Rioult et al. 1997) suggests that it would be wise to continue considering an Aalenian age (Concavum Zone) or, preferably, a Concavum-Discites age interval for the sediments immediately below the volcanic deposit in SA.1-1, PI-BA.1-5, and PI-BA.1-7 sections.

Because the volcanic activity can generate mounds and they can acquire an early cemented condition, their flanks will be progressively onlapped by sediments younger than the volcanic deposits until fully cover them. Hence, the ages of post-volcanic sediments have proved to be quite variable depending upon the locality where the sampling is performed. Bathonian or Callovian sediments (Domeño Formation) directly cover volcanic rocks 44 m thick in the CA-31 section, whereas a volcanic pile 37 m thick is overlain by Bajocian beds (Moscardón Formation) in the CA-35 section (Fig. 4).

Looking for pinch-out zones of volcanic cones, where the thickness vanishes, is crucial to determine the age of their stratigraphic emplacements and to detect sedimentary hiatuses. The ammonite assemblage found in the post-volcanic sedimentary bed of the PI-BA.1-7 section (Fig. 5) shows taphonomic condensation evidenced by a mixture of reelaborated elements representing different chronostratigraphic units. Based on the stratigraphic distribution of Bajocian ammonite taxa stated by Fernández-López (1985), the fossil assemblage could be indicating an age that corresponds to the Laeviuscula-Propinquans interval for the bed containing it.

The PI-BA.2-4 (Fig. 3), CA-1 (Fig. 4), and SA.2-1 (Fig. 6) sections are more clarifying, since they allow strongly narrowing the possible limit of the upper age of the volcanic deposit. Nevertheless, none of the post-volcanic ammonite assemblages from these three sections resolves the uncertainty of whether they are Aalenian (Concavum Zone) or Bajocian (Discites Zone) in age. As was the case in the pre-volcanic ammonite assemblages, occurrences of the biochronologic marker of the Discites Zone (genus *Hyperlioceras* or *Hyperlioceras-Toxolioceras* group) are still lacking. The genera *Braunsina* and *Reynellesa* recorded at the top of the post-volcanic interval in the PI-BA.2-4 (Fig. 3) are certainly not present in pre-volcanic assemblages; however, they have been reported to occurr both in the upper part of the Aalenian Concavum Zone (Limitatum Subzone) and in the Bajocian Discites Zone in Jurassic successions of the Iberian Range (García-Frank 2006). By contrast, the genus *Graphoceras* persists, along with the genera *Reynesella* and *Braunsina*, above the volcanic deposit in the PI-BA.2-4 section (Fig. 3). However, the last occurrences of the genus *Graphoceras* may also extend into the Bajocian Discites Zone (García-Frank 2006).

Although the Concavum and Discites zones cannot be discriminated from the post-volcanic fossil content, these assemblages constrain the age of the volcanic stratigraphic position. An Aalenian age (Concavum Zone) or, preferably, a Concavum-Discites age interval for the post-volcanic sediments in CA-1, PI-BA.2-4, and SA.2-1 sections should be considered.

In addition, a specimen of *Fontannesia grammoceroides* (r) (Fig. 12B) has been found in a cross-bedded volcano-sedimentary lithofacies from the upper part of the volcanic pile near the SA.2-1 section. It is an unusual internal mold, only rarely produced and preserved, since it is comprised by fine-grained epiclastic material. This taxon has frequently been found in the Bajocian Discites Zone (e.g., Fernández-López et al. 1988; Rocha et al. 1990; Linares & Sandoval 1990; Chandler & Sole 1995; Rioult et al. 1997), although it has also been cited in the upper part of the Aalenian Concavum Zone (e.g., Pavia & Martire 1997). As the process of fossilization required the previous existence of uncemented -and not covered by sediments yet- volcanic accumulations in the submarine floor, the range of age in which the volcanic deposit could have been recorded is again ratified. Therefore, as already pointed out by Cortés & Gómez (2016), the age of the volcanic episode V_{12} would tie in well with the Concavum-Discites zonal boundary.

Volcanic episode V_{13}. This episode is interbedded in the lower-middle part of the El Pedregal Formation, and it occurs exclusively restricted to the Alcublas Fault Zone (LLÍR-5, AB-2, and AB-3 stratigraphic sections, Fig. 1A).

The last and most recent ammonite assemblage found below the base of the volcanic deposit in the LLÍR-5 section [*Sonninites corrugatus* (r), *Pelekodites* sp. (r), *Witchellia* sp. (r), *Witchellia romanoides* (r), *Witchellia rubra* (r), and *Witchellia* gr. *laeviuscula* (r)] (Fig. 7) characterizes the Bajocian Laeviuscula Zone. However, although most of these species can extend into the Propinquans Zone, reliable key indicators of this zone are still absent (according to Fernández-López 1985). An almost 2 m thick stretch, with no ammonite records and partially covered, separates the mentioned ammonite assemblage from the volcanic base, so there is a possibility that the Propinquans chronorecords could be lodged in this stretch.

In the AB-2 section (Fig. 8), *Mollistephanus* sp. (r) has been obtained about 4 meters below the volcanic base, probably identifying the Laeviuscula Zone. The ammonite species of sediments overlying the volcanic deposit are characteristic of the Bajocian Propinquans Zone, according to the biochronostratigraphic distribution of Bajocian ammonites in Fernández-López (1985).

In the AB-3 section (Fig. 8), wherever the thickness of the volcanic accumulation has strongly thinned, the immediately pre-volcanic beds include *Papilliceras* sp. (r), *Sonninites corrugatus* (r), and *Pelekodites* sp. (r), which unquestionably characterize the Laeviuscula Zone, being able to extend into the Propinquans Zone (according to Fernández-López 1985). However, as happened in the LLÍR-5 section, no key markers of the Propinquans Zone have occurred. Above the volcanic top appeared *Stephanoceras* sp. (r), *Nannina* sp. (r), and *Dorsetensia* sp. (r), which characterize the Propinquans Zone, according to Fernández-López (1985).

Based on the foregoing, it is inferred that the volcanic episode V_{13} is early Bajocian (Laeviuscula Zone) in age, although an age about the Laeviuscula-Propinquans zonal boundary could also be acceptable.

Time correlation between volcanic episodes and volcanism

Volcaniclastic submarine edifices accumulated in shallow seas are highly prone to be reworked and may be subjected to varying degrees of denudation, especially before early cementation. It means that the volcanic piles could be: 1) partially eroded, with portions of material being moved towards the most distal parts of the mounds or displaced beyond their limits, 2) completely dismantled, although residual deposits can remain as the only evidence of previous volcanic edifices.

The isolated epiclastic beds -both vestigial and cut off from the still-present primary volcanic stacks- might be redeposited either on a coeval seafloor or on substrates more recent than those on which they were primarily deposited. Therefore, certain epiclastic volcanic levels could not match volcanic events.

Non-reworked lava flows and pyroclastic deposits are among the most reliable estimators of primary erupted material. Lava flows have been reported in the episode V_{12} of the CA-31 (Fig. 4) and the SA.1-1 (Fig. 6) sections. Original pyroclastic deposits can be observed in all three volcanic episodes: V_{11} in the CAM.1-2 section (Fig. 3), V_{12} in the CA-31 and CA-35 (Fig. 4), PI-BA.1-5 (Fig. 5), and SA.1-1 (Fig. 6) sections, and V_{13} in the LLÍR-5 (Fig. 7) and AB-2 (Fig. 8) sections.

The length/height ratio very often confers a mound morphology to the Middle Jurassic volcanic deposits, which persists over a long time if the volcanics are early cemented. The presence of subaqueous clastic mounds and cones constitute reliable diagnostic clues for the recognition of primary volcanic events, since no edifice having a positive relief can be formed entirely from reworked volcanic deposits (White et al. 2003). Mound morphologies have been identified in the volcanic episode V_{11} (CAM.1-2 and CAM.1-5 sections, Fig. 3), in the episode V_{12} (CA-1, CA-31, and CA-35 sections, Fig. 4; PI-BA.1-5 and PI-BA.1-7 sections, Fig. 5; SA.1-1 and SA.2-1 sections, Fig. 6), and in the episode V_{13} (AB-2 and AB-3 sections, Fig. 8).

Therefore, all this information shows that the estimated ages for the volcanic episodes interbedded in the sedimentary successions evidence times of volcanic activity during the Middle Jurassic in the Iberian platform system.

Coeval volcanism in the Iberian Plate

As Cortés (2020a) stated, the Lower Jurassic volcanic activity in the eastern paleomargin of

Iberia also took place in its southern paleomargin. Likewise, compositionally comparable magmatic events were recorded in both areas during the early Middle Jurassic (García-Yebra et al. 1972; García-Hernández et al. 1980; Ancochea et al. 1988; Vera 1988, 2001; Molina & Vera 2001; Puga et al. 2004; Cortés 2018). Effusive lavas and pillow lavas, along with subvolcanic dikes and sills, prevailed across the Median Subbetic (Gómez et al. 2019) over the predominantly explosive volcanism that occurred in the Iberian platforms (Cortés 2018). The onset of multiple processes, such as the rifting and spreading of the Alpine Ocean, the fragmentation of the Iberian and Betic platforms, and the magmatism, was roughly synchronous about the late Pliensbachian (Vera et al. 2004; Gómez et al. 2019; Cortés 2020a), whereas the end of the magmatic processes was diachronous. The last volcanic episode has been dated as early Bajocian (late Laeviuscula Zone or Laeviuscula-Propinquans zonal boundary) in the Iberian platform system (Cortés 2018, this work). However, the igneous appearances greatly exceeded the Jurassic times in the Median Subbetic, with volcanic episodes that persisted until the Cretaceous (Santonian) times (Molina et al. 1998; Molina & Vera 2008).

Volcanism and active faulting during the Middle Jurassic passive-margin stage

Traditional rifting models consider the post-rifting or passive margin stages as being seismically inactive, tectonically quiescent, and with poor or inexistent magmatic activity. The Iberian Basin, and, therefore, the eastern Iberian paleomargin where the studied area is included, spent the Middle Jurassic under a passive margin stage (Salas & Casas 1993; Salas et al. 2001; Gómez et al. 2019). Nevertheless, faulting, non-uniform subsidence, and volcanism occurred. The specific threshold of cortical stretching required to regard this period as a rifting interval may not have been exceeded. However, Fernández-López & Gómez (2004) and Gómez & Fernández-López (2006) reported the existence of depocenters and sedimentary highs, controlled by NW-SE and NE-SW trending normal faults, in the Middle Jurassic eastern platform system. Some of these faults influenced the location of restricted and open marine facies across the Castilian-Valencian Iberian platform, such as the Montes Universales –or the Alto Tajo-Montes Universales, according to Aurell et al. (2019)– and the Castellón faults. Moreover, the Middle Jurassic volcanic outcrops appear aligned across three of the mentioned NW-SE and NE-SW structures (the Teruel, Caudiel, and Alcublas fault zones), thus emphasizing the relevant role of faulting in the volcanic product release (Cortés & Gómez 2016; Cortés 2018).

Both angular unconformities and block tilting related to Middle Jurassic volcanism have been reported by Santisteban (2016, 2018) in the Teruel and Valencia domains. Aurell et al. (2019) suggest that the transition from the thermal-dominated subsidence during the Middle Jurassic to the Upper Jurassic-Lower Cretaceous rifting stage (fault-controlled subsidence) was progressive rather than abrupt since fault-bounded depocenters and volcanism could be considered either as the immediately rifting prelude or already as rifting features.

Conclusions

1) The study of time-marker fossil assemblages, mainly ammonites, have made it possible to identify three episodes of volcanic rocks of different ages interbedded within the Middle Jurassic sedimentary successions (lower and middle parts of the El Pedregal Formation) in the southeastern area of the Iberian Range. These episodes have been numbered V_{11}, V_{12}, and V_{13}, from oldest to youngest, following the first 10 previous volcanic episodes included in the Lower Jurassic sedimentary successions across the same studied area. The detailed ages of the volcanic phases are as follows: V_{11} (Aalenian Murchisonae Zone), V_{12} (Aalenian Concavum-Bajocian Discites zonal boundary), and V_{13} (Bajocian late Laeviuscula Zone or Bajocian Laeviuscula-Propinquans zonal boundary).

2) The volcanic outcrops follow NW-SE and NE-SW (or NNE-SSW) fault-zone alignments. The igneous rocks are arranged along three main fault zones known as the Teruel Fault Zone (NE-SW or NNE-SSW), and the Caudiel and Alcublas fault zones (NW-SE). The oldest volcanic phase V_{11} is mainly located in the northern part of the Teruel Fault Zone, where the Teruel and Caudiel fault zones intersect, and, sporadically, in the Caudiel Fault. The volcanic phase V_{12} is restricted to the Caudiel Fault Zone, while the youngest V_{13} is only exposed in the Alcublas Fault Zone.

3) A coeval volcanism, comparable in composition, was also recorded in the Median Subbetic domain of the Betic Cordillera. However, more effusive eruptions predominated in the Subbetic against the almost totally explosive character that took place in the Iberian platforms. The igneous activity ended in the early Bajocian (late Laeviuscula Zone or Laeviuscula-Propinquans zonal boundary) in the Iberian platform system, whereas the magmatism lasted until Cretaceous (Santonian) times in the Median Subbetic Basin.

4) This study sheds new light on the age of the magmatism occurring over a time interval during the Alpine Cycle in Iberia. The results drawn from this work may provide a tool to reconstruct the geotectonic evolution of the eastern Iberian paleomargin in the western Tethys during Middle Jurassic times. Moreover, future studies on alternative geological disciplines may benefit from the outcomes after the formerly known in a broad sense as "Jurassic volcanism" has been subdivided, differentiated, and accurately dated. Sampling will lead to the most appropriate conclusions when the precise age of the samples is known.

Acknowledgments: This work would not have been possible without the taxonomic determinations, valuable clarifications, support, suggestions, and contributions of professors Antonio Goy, Sixto Fernández López, Soledad Ureta (Complutense University of Madrid), and José Sandoval (University of Granada). I would also like to acknowledge the constructive reviews and suggestions of two anonymous reviewers and the helpful comments and editorial handling of Fabrizio Berra, Lucia Angiolini and Cristina Lombardo, which have greatly improved the quality of the initial manuscript. Finally, thanks to Raquel Fuertes, Msc for the language proofreading and corrections.

References

Ancochea E., Muñoz M. & Sagredo J. (1988) - Identificación geoquímica del vulcanismo Jurásico de la Cordillera Ibérica. *Geociências (Aveiro)*, 3(1-2): 15-22.

Aurell M., Robles S., Bádenas B., Rosales I., Quesada S., Meléndez G. & García-Ramos J.C. (2003) - Transgressive-regressive cycles and Jurassic palaeogeography of northeast Iberia. *Sedimentary Geology*, 162(3-4): 239-271. https://doi.org/10.1016/s0037-0738(03)00154-4

Aurell M., Fregenal-Martínez M., Bádenas B., Muñoz-García M.B., Élez J., Meléndez N. & de Santisteban C. (2019) - Middle Jurassic-Early Cretaceous tectono-sedimentary evolution of the southwestern Iberian Basin (central Spain): Major palaeogeographical changes in the geotectonic framework of the Western Tethys. *Earth-Science Reviews*, 199: 102983. https://doi.org/10.1016/j.earscirev.2029.102983

Baeza-Carratalá J.F., García Joral F. & Tent-Manclús J.E. (2016) - Lower Jurassic brachiopods from the Ibero-Levantine Sector (Iberian Range): Faunal turnovers and critical bioevents. *Journal of Iberian Geology*, 42(3): 355-369. https://doi.org/10.5209/jige.54666

Bakx L.A.J. (1935) - La géologie de Cascante del Río et de Valacloche (Espagne). *Leidsche Geologische Mededeelingen*, 7(2): 157-220.

Blakey R. (2011) - Paleogeography of Europe Series. Deep Time Maps. Retrieved October 20, 2020, from https://www.deeptimemaps.com/map-room/

Bulard P.F. (1971) - La discontinuité entre le Callovien et l'Oxfordien sur la bordure nord-est des Chaînes Ibériques. *Cuadernos de Geología Ibérica*, 2: 425-438.

Chandler R.B. & Sole D.T.C. (1995) - The Inferior Oolite at East Hill Quarry, Bradford Abbas, Dorset. *Proceedings of the Dorset Natural History and Archaeological Society*, 117: 101-108.

Cohen K.M., Finney S.C., Gibbard P.L. & Fan J.-X. (2013; updated) - The ICS International Chronostratigraphic Chart. *Episodes*, 36(3): 199-204. https://stratigraphy.org/chart

Cortés J.E. (2018) - La arquitectura deposicional de los carbonatos del Jurásico Inferior y Medio relacionados con los materiales volcánicos del sureste de la Cordillera Ibérica. PhD Thesis, Universidad Complutense de Madrid, 1272 pp.

Cortés J.E. (2020a) - Volcanic rocks in Lower Jurassic marine carbonate successions in the southeastern Iberian Range (Spain): biochronostratigraphic dating. *Journal of Iberian Geology*, 46(3): 253-277.https://doi.org/10.1007/s41513-020-00134-z

Cortés J.E. (2020b) - Interaction between volcanism, tectonics and sedimentation in a shallow carbonate platform: a case study from the western Tethys (Middle Jurassic, southeastern Iberian Range). *Estudios Geológicos*, 76(1): e129. https://doi.org/10.3989/egeol.43590.537

Cortés J.E. & Gómez J.J. (2016) - Middle Jurassic volcanism in a magmatic-rich passive margin linked to the Caudiel Fault Zone (Iberian Range, East of Spain): biostratigraphical dating. *Journal of Iberian Geology*, 42(3): 335-354. https://doi.org/10.5209/JIGE.54667

Cortés J.E. & Gómez J.J. (2018) - The epiclastic barrier-island system of the Early-Middle Jurassic in eastern Spain). *Journal of Iberian Geology*, 44(2): 257-271. https://doi.org/10.1007/s41513-018-0061-7

De Santisteban C. (2016) - La fracturación de la rampa carbonática del tránsito Jurásico Inferior a Medio y volcanismo asociado en el sector de La Salada (Sistema Ibérico, Teruel). *Geogaceta*, 60: 3-6.

De Santisteban C. (2018) - El volcanismo de La Concòrdia (Llíria, Valencia) y las discontinuidades adyacentes al límite Jurásico Inferior-Jurásico Medio, en el sector Suroriental del Surco Ibérico. *Geogaceta*, 63: 23-26.

Fernández-López S. (1984a) - Nuevas perspectivas de la tafonomía evolutiva: Tafosistemas y asociaciones conservadas. *Estudios Geológicos*, 40(3-4): 215-224. https://doi.org/10.3989/egeol.84403-4662

Fernández-López S.(1984b) - Criterios elementales de reelaboración tafonómica en ammonites de la Cordillera Ibérica. *Acta Geológica Hispánica*, 19(2): 105-116.

Fernández-López S.R. (1985) - El Bajociense en la Cordillera Ibérica. I. Taxonomía y sistemática (Ammonoidea). II. Bioestratigrafía. III. Atlas. PhD Thesis, Universidad Complutense de Madrid, 850 pp.

Fernández-López S. (1986) - Sucesiones paleobiológicas y sucesiones registráticas (nuevos conceptos paleontológicos). *Revista Española de Paleontología*, 1: 29-45.

Fernández-López S. (1997) - Ammonites, taphonomic cycles and stratigraphic cycles in carbonate epicontinental platforms. *Cuadernos de Geología Ibérica*, 23: 95-136.

Fernández-López S. & Gómez J.J. (2004) - The Middle Jurassic Eastern margin of the Iberian platform system (eastern Spain). Palaeogeography and biodispersal routes of ammonoids. *Rivista Italiana di Paleontologia e Stratigrafia*, 110(1): 151-162. https://doi.org/10.13130/2039-4942/6281

Fernández-López S., Gómez J.J. & Goy A. (1985) - Sédimentologie des carbonates développés sur un "monticule" de matériaux volcaniques. In: Canerot J. & Goy A. (Eds.) - Le Jurassique des Ibérides Orientales (Espagne). *Strata*, *serie 2: mémoires*, vol. 2: 101-115.

Fernández-López S., Henriques M.H., Mouterde R., Rocha R. & Sadki D. (1988) - Le Bajocien inférieur du Cap Mondego (Portugal) - Essai de biozonation. In: Rocha R.B. & Soares A.F. (Eds.) - 2nd International Symposium on Jurassic Stratigraphy: 301-313. Centro de Estratigrafia e Paleobiologia da Universidade Nova de Lisboa, Lisbon.

Fisher R.V. & Schmincke H.-U. (1984) - Pyroclastic rocks. Springer-Verlag, Berlin, 472 pp. https://doi.org/10.1007/978-3-642-74864-6

García-Frank A. (2006) - Evolución biosedimentaria y secuencial del Jurásico Medio inferior en la Cuenca Ibérica (Sector NO). PhD Thesis, Universidad Complutense de Madrid, 529 pp.

García-Frank A., Ureta S. & Mas R. (2006) - Tectonically active Aalenian in the northwestern Iberian Basin (Spain). 7th International Congress on the Jurassic System, Poland-Kraków. *Volumina Jurassica*, IV: 42.

García-Frank A., Ureta S. & Mas R. (2008) - Aalenian pulses of tectonic activity in the Iberian Basin, Spain. *Sedimentary Geology,* 209(1-4): 15-35. https://doi.org/10.1016/j.sedgeo.2008.06.004

García-Hernández M., López-Garrido A.C., Rivas P., Sanz de Galdeano C. & Vera J.A. (1980) - Mesozoic palaeogeographic evolution of the External Zones of the Betic Cordillera. *Geologieen Mijnbouw*, 59(2): 155-168.

García Joral F. & Goy A. (2000) - Stratigraphic distribution of Toarcian brachiopods from the Iberian Range (Spain) and its relation to depositional sequences. In: Hall R.L. & Smith P.L. (Eds.) - Advances in Jurassic Research 2000. Proceedings of the Fifth International Symposium on the Jurassic System, Vancouver. *GeoResearch Forum*, 6: 381-386.

García Joral F., Gómez J.J. & Goy A. (2011) - Mass extinction and recovery of the Early Toarcian (Early Jurassic) brachiopods linked to climate change in Northern and Central Spain. *Palaeogeography*, *Palaeoclimatology*, *Palaeoecology*, 302(3-4): 367-380. https://doi.org/10.1016/j.palaeo.2011.01.023

García Joral F., Andrade B., Baeza-Carratalá J.F., Colás J., Comas-Rengifo M.J., Goy A. & Rodrigo A. (2016) - Los rinconélidos (Brachiopoda, Rhynchonellida) del Jurásico Inferior de España: Distribución estratigráfica y elementos de correlación. In: Meléndez G., Núñez A. & Tomás M. (Eds.) - Actas de las XXXII Jornadas de la Sociedad Española de Paleontología, Molina de Aragón (Guadalajara). *Cuadernos del Museo Geominero*, 20: 61-66.

García-Yebra R., Rivas P. & Vera J.A. (1972) - Precisiones sobre la edad de las coladas volcánicas jurásicas en la región Algarinejo-Lojilla (Zona Subbética). *Acta Geológica Hispánica*, VII (5): 133-137.

Gautier F. (1968) - Sur l'existence et l'age d'un paléovolcanisme dans le Jurassique sud-aragonais (Espagne). *Compte Rendu Sommaire des Séances de la Société Géologique de France*, 3: 74-75.

Gautier F. & Odin G.S. (1985) -Volcanisme Jurassique du sud de l'Aragon (Espagne). *Bulletin de Liaison et Information*, *I.G.C.P. Project 196, offset Paris*, 5: 34-38.

Gómez J.J. (1979) - El Jurásico en facies carbonatadas del sector levantino de la Cordillera Ibérica. Seminarios de Estratigrafía, Serie Monografías 4. Universidad Complutense de Madrid-Consejo Superior de Investigaciones Científicas, Madrid, 683 pp.

Gómez J.J. & Fernández-López S. (1994) - Condensed processes in shallow platforms. *Sedimentary Geology*, 92(3-4): 147-159. https://doi.org/10.1016/0037-0738(94)90103-1

Gómez J.J. & Fernández-López S. (2004) - Las unidades litoestratigráficas del Jurásico Medio de la Cordillera Ibérica. *Geogaceta*, 35:91-94.

Gómez J.J. & Fernández-López S. (2006) - The Iberian Middle Jurassic carbonate-platform system: Synthesis of the palaeogeographic elements of its eastern margin (Spain). *Palaeogeography, Palaeoclimatology, Palaeoecology*, 236(3-4): 190-205. https://doi.org/10.1016/j.palaeo.2005.11.008

Gómez J.J. & Goy A. (1977) - Estudio de las facies relacionadas con un montículo de origen volcánico en el Jurásico Medio de Caudiel (Castellón). VIII Congreso Nacional de Sedimentología, Oviedo-León. Resumen de Comunicaciones Científicas.

Gómez J.J. & Goy A. (1979) - Las unidades litoestratigráficas del Jurásico medio y superior en facies carbonatadas del Sector Levantino de la Cordillera Ibérica. *Estudios Geológicos*, 35: 569-598.

Gómez J.J. & Goy A. (2000) - Definition and organization of limestone-marl cycles in the Toarcian of the northern and east-central part of the Iberian Subplate (Spain). In: Hall R.L. & Smith P.L. (Eds.) - Advances in Jurassic Research 2000. Proceedings of the Fifth International Symposium on the Jurassic System, Vancouver. *GeoResearch Forum*, 6: 301-310.

Gómez J.J. & Goy A. (2005) - Late Triassic and Early Jurassic palaeogeographic evolution and depositional cycles of the Western Tethys Iberian platform system (East-

ern Spain). *Palaeogeography, Palaeoclimatology, Palaeoecology*, 222(1-2): 77-94. https://doi.org/10.1016/j.palaeo.2005.03.010

Gómez J.J., Trell A. & Pérez P. (1976) - Presencia y edad de vulcanitas en el Jurásico del Norte de Valencia (Cordillera Ibérica, España). *Acta Geológica Hispánica*, 1: 1-7.

Gómez J.J., Comas-Rengifo M.J. & Goy A. (2003) - Las unidades litoestratigráficas del Jurásico Inferior de las Cordilleras Ibérica y Costeras Catalanas. *Revista de la Sociedad Geológica de España*, 16(3-4): 227-238.

Gómez J.J., Fernández-López S. & Goy A. (2004) - Primera fase de post-rifting: Jurásico Inferior y Medio. In: Vera J.A. (Ed.) - Geología de España: 495-503. Sociedad Geológica de España-Instituto Geológico y Minero de España (SGE-IGME), Madrid.

Gómez J.J., Aguado R., Azerêdo A.C., Cortés J.E., Duarte L.V., O'Dogherty L., Bordalo da Rocha R. & Sandoval J. (2019) - The Late Triassic-Middle Jurassic Passive Margin Stage. In: Quesada C. & Oliveira J.T. (Eds.) - The Geology of Iberia: A Geodynamic Approach. The Alpine Cycle (Vol. 3): 113-167. Springer, Berlin. https://doi.org/10.1007/978-3-030-11295-0_4

Goy A. & Martínez G. (1990) - Biozonación del Toarciense en el área de La Almunia de Doña Godina-Ricla (Sector Central de la Cordillera Ibérica). *Cuadernos de Geología Ibérica*, 14: 11-53.

Henriques M.H., Linares A., Sandoval J. & Ureta M.S. (1996) - The Aalenian in the Iberia (Betic, Lusitanian and Iberian Basins). *GeoResearch Forum*, 1-2: 139-150.

Lago M., Arranz E., Pocoví A., Martínez R.M., Gil-Imaz A., Valenzuela-Ríos J.I. & García J. (1996) - Contribución de los magmatismos presentes en la Comunidad Autónoma de Aragón al Patrimonio Geológico. *Geogaceta*, 20(5): 1175-1176.

Lago M., Arranz E., Gil A. & Pocoví A. (2004) - Magmatismo asociado. In: Vera J.A. (Ed.) - Geología de España: 522-525. Sociedad Geológica de España-Instituto Geológico y Minero de España (SGE-IGME), Madrid.

Linares A. & Sandoval J. (1990) - The Lower boundary of the Bajocian in the "Barranco de Agua Larga" section (Subbetic Domain, Southern Spain). Memorie Descrittive della Carta Geologica d'Italia, XL: 13-22.

Martin R. (1936) - Die geologie von Camarena de la Sierra und Riodeva (Provinz Teruel, Spanien). *Leidsche Geologische Mededeelingen*, 8(1):55-154.

Martínez R.M., Lago M., Valenzuela J.I., Vaquer R. & Salas R. (1996a) - El magmatismo alcalino jurásico del sector SE de la Cadena Ibérica: Composición y estructura. *Geogaceta*, 20(7): 1687-1690.

Martínez R.M., Lago M., Vaquer R., Arranz E. & Valenzuela J.I. (1996b) - Precisiones terminológicas entre mecanismos de fragmentación y emplazamiento de rocas volcanoclásticas. *Geogaceta*, 20(3): 515-517.

Martínez R.M., Lago M., Vaquer R., Valenzuela J.I. & Arranz E. (1996c) - Composición mineral del volcanismo jurásico (pre-Bajociense medio) en la Sierra de Javalambre (Cordillera Ibérica, Teruel): Datos preliminares. *Geogaceta*, 19: 41-44.

Martínez R., Valenzuela J.I., Lago M., Vaquer R. & Arranz E. (1996d) - Las rocas volcanoclásticas jurásicas de Albentosa-1 (Cordillera Ibérica, Teruel): Mecanismos de fragmentación y emplazamiento. *Geogaceta*, 19: 45-46.

Martínez R.M., Lago M., Valenzuela J.I., Vaquer R., Salas R. & Dumitrescu R. (1997a) - El volcanismo Triásico y Jurásico del sector SE de la Cadena Ibérica y su relación con los estadios de rift mesozoicos. *Boletín Geológico y Minero*, 108-4 and 5 (367-376): 39-48.

Martínez R.M., Valenzuela J.I., Lago M., Bastida J. & Vaquer R. (1997b) - Origen epiclástico de estratificaciones cruzadas afectando a materiales volcanoclásticos jurásicos en la Sierra de Javalambre (Teruel). *Cuadernos de Geología Ibérica*, 22: 121-137.

Martínez R.M., Vaquer R. & Lago M. (1998) - El volcanismo jurásico de la Sierra de Javalambre (Cadena Ibérica, Teruel). *Teruel*, 86(1): 43-61.

Martínez-González R.M., Lago M., Valenzuela-Ríos J.I. & Arranz E. (1996) - Interés como Patrimonio Geológico de dos magmatismos mesozoicos en la Sierra de Javalambre (Teruel). *Geogaceta*, 20(5): 1186-1188.

McPhie J., Doyle M. & Allen R. (1993) - Volcanic textures. A guide to the interpretation of textures in volcanic rocks. Centre for Ore Deposit and Exploration Studies (CODES Key Centre), University of Tasmania, Tasmania, 196 pp.

Molina J.M. & Vera J.A. (2001) - Interaction between sedimentation and submarine volcanism (Jurassic, Subbetic, southern Spain). *Geogaceta*, 29: 142-145.

Molina J.M. & Vera J.A. (2008) - Resedimented carbonate and volcanic rocks in the Berriasian-Hauterivian of the Subbetic (Alamedilla, Betic Cordillera, southern Spain). *Cretaceous Research*, 29(5-6): 781-789. https://doi.org/10.1016/j.cretres.2008.05.023

Molina J.M., Vera J.A. & de Gea G. (1998) - Vulcanismo submarino del Santoniense en el Subbético: Datación con nannofósiles e interpretación (Formación Capas Rojas, Alamedilla, Provincia de Granada). *Estudios Geológicos*, 54(5-6): 191-197. https://doi.org/10.3989/egeol.98545-6218

Neige P. & Rouget I. (2002) - Les ammonites du Toarcien de Chantonnay (Vendée, France): analyse paléontologique, biostratigraphie et réflexion sur les Hildoceratinae. *Geodiversitas*, 24(4): 765-784.

Neige P. & Rouget I. (2015) - Evolutionary trends within Jurassic ammonoids. In: Klug C., Korn D., de Baets K., Kruta I. & Mapes R.H. (Eds.) - Ammonoid paleobiology: from macroevolution to paleogeography. *Topics in Geobiology,* 44: 51-66. Springer, Berlin. https://doi.org/10.1007/978-94-017-9633-0

Odin G.S., Desprairies A., Fullagar P.D., Bellon H., Decarreau A., Fröhlich F. & Zelvelder M. (1988) - Nature and geological significance of celadonite. In: Odin G.S. (Ed.) - Green marine clays. *Developments in Sedimentology,* 45: 337-398. Elsever, Amsterdam. https://doi.org/10.1016/s0070-4571(08)70071-2

Ortí F. (1987) - La zona de Villel-Cascante-Javalambre. Introducción a las formaciones evaporíticas y al volcanismo

jurásico. In: Gutiérrez. M & Meléndez A. (Eds.) - Libro del XXI Curso de Geología Práctica de Teruel: 53-92. Universidad de verano de Teruel.

Ortí F. & Sanfeliu T. (1971) - Estudio del vulcanismo jurásico de Caudiel (Castellón) en relación con procesos de lateritización, condensación y silicificación de la serie calcárea. Instituto de Investigaciones Geológicas de la Diputación Provincial. Barcelona, vol. XXVI: 21-34.

Ortí F. & Vaquer R. (1980) - Volcanismo jurásico del sector valenciano de la Cordillera Ibérica. Distribución y trama estructural. *Acta Geológica Hispánica*, 15(5): 127-130.

Osete M.L., Gómez J.J., Pavón-Carrasco F.J., Villalaín J.J., Palencia-Ortas A., Ruiz-Martínez V.C. & Heller F. (2011) - The evolution of Iberia during the Jurassic from palaeomagnetic data. *Tectonophysics*, 502(1-2): 105-120. https://doi.org/10.1016/j.tecto.2010.05.025

Page K. N. (2003) - The Lower Jurassic of Europe: its subdivision and correlation. *Geological Survey of Denmark and Greenland Bulletin*, 1: 23-59. https://doi.org/10.34194/geusb.v1.4646

Palencia A., Osete M.L., Martínez-González R. & Martín-Hernández F. (2000) - Estudio paleomagnético del volcanismo jurásico de la región de Javalambre. 2ª Assembleia Luso-Espanhola de Geodesia e Geofísica. Abstracts: 333-334, Lagos (Portugal).

Palencia-Ortas A. (2000) - Estudio paleomagnético en rocas de edad Jurásico Inferior-Medio de la placa Ibérica. Tesis de Licenciatura, Universidad Complutense de Madrid, 125 pp.

Pavia G. & Fernández-López S. (2016) - *Pseudoteloceras*, a new stephanoceratid genus (Ammonitida) of the lower Humphriesianum Zone (lower Bajocian, Middle Jurassic) from western Tethys. *Proceedings of the Geologists' Association*, 127(2): 196-209. https://doi.org/10.1016/j.pgeola.2015.12.006

Pavia G. & Fernández-López S. (2019) - Bajocian Lissoceratinae (Haploceratoidea, Ammonitida) from the Mediterranean-Caucasian Subrealm. *Rivista Italiana di Paleontologia e Stratigrafia*, 125(1): 29-75.

Pavia G. & Martire L. (1997) - The importance of taphonomic studies on biochronology: examples from the european Middle Jurassic. *Cuadernos de Geología Ibérica*, 23: 153-181.

Puga E., Morata D. & Díaz de Federico A. (2004) - Magmatismo mesozoico y metamorfismo de muy bajo grado. In: Vera J.A. (Ed.) - Geología de España: 386-387. Sociedad Geológica de España-Instituto Geológico y Minero de España (SGE-IGME), Madrid.

Quesada C. & Oliveira J.T. (2019) - Preface. In: Quesada C. & Oliveira J.T. (Eds.) - The Geology of Iberia: A Geodynamic Approach. The Alpine Cycle (Vol. 3): xvii-xix. Springer, Berlin. https://doi.org/10.1007/978-3-030-11295-0

Rioult M., Contini D., Elmi S., Gabilly J. & Mouterde R. (1997) - Bajocien. In: Cariou E. & Hantzpergue P. (Coord.) - Biostratigraphie du Jurassique ouest-européen et meéditerranéen: zonations parallèles et distribution des invertébrés et microfossiles. *Bulletin du Centre de Recherches Elf Exploration Production*, *Mémoir* 17: 41-53.

Rocha R.B., Henriques M.H., Soares A., Mouterde R., Caloo B., Ruget C. & Fernández-López S. (1990) - The Cabo Mondego section as a possible Bajocian boundary stratotype. Memorie Descrittive della Carta Geologica d'Italia, XL: 49-60.

Rulleau L. (2010) - La biodiversité en Paléontologie. *Bulletin de la Société linnéenne de Lyon, hors-série*, 2: 20-22. https://doi.org/10.3406/linly.2010.13740

Salas R. & Casas A. (1993) - Mesozoic extensional tectonics, stratigraphy and crustal evolution during the Alpine cycle of the eastern Iberian basin. *Tectonophysics*, 228(1-2): 33-55. https://doi.org/10.1016/0040-1951(93)90213-4

Salas R., Guimerà J., Mas R., Martín-Closas C., Meléndez A. & Alonso A. (2001) - Evolution of the Mesozoic Central Iberian Rift System and its Cainozoic inversión (Iberian Chain). In: Ziegler P.A., Cavazza W., Robertson A.H.F. & Crasquin-Soleau S. (Eds.) - Peri-Tethys Memoir 6: Peri-Tethyan rift/wrench basins and passive margins. *Mémoires du Muséum National d'Histoire Naturelle*, 186: 145-186.

Sandoval J., Henriques M.H., Ureta S., Goy A. & Rivas P. (2001) - The Lias/Dogger boundary in Iberia: Betic and Iberian cordilleras and Lusitanian basin. *Bulletin de la Société Géologique de France*, 172(4): 387-395.

Schettino A. & Turco E. (2011) - Tectonic history of the western Tethys since the Late Triassic. *Geological Society of American Bulletin*, 123(1-2): 89-105. https://doi.org/10.1130/b30064.1

Sohn C. & Sohn Y.K. (2019) - Distinguishing between primary and secondary volcaniclastic deposits. *Scientific Reports*, 9: 12425. https://doi.org/10.1038/s41598-019-48933-4

Ureta S., Goy A., Gómez J.J. & Martínez G. (1999) - El límite Jurásico Inferior-Jurásico Medio en la sección de Moyuela (Zaragoza, España). *Cuadernos de Geología Ibérica*, 25: 59-71.

Valenzuela J.I., Martínez R.M. & Lago M. (1996) - Nota preliminar sobre la edad del paleovolcanismo jurásico de Javalambre (Cordillera Ibérica, Teruel). *Geogaceta*, 19: 39-40.

Vera J.A. (1988) - Evolución de los sistemas de depósito en el margen ibérico de la Cordillera Bética. *Revista de la Sociedad Geológica de España*, 1(3-4): 373-391.

Vera J.A. (2001) - Evolution of the South Iberian Continental Margin. In: Ziegler P.A., Cavazza W., Robertson A.H.F. & Crasquin-Soleau S. (Eds.) - Peri-Tethys Memoir 6: Peri-Tethyan rift/wrench basins and passive margins. *Mémoires du Muséum National d'Histoire Naturelle*,186: 109-143.

Vera J.A., Arias C., García-Hernández M., López-Garrido A.C., Martín-Algarra A., Martín-Chivelet A., Molina J.M., Rivas P., Ruiz-Ortiz P.A., Sanz de Galdeano C. & Vilas L. (2004) - Las Zonas Externas Béticas y el Paleomargen Sudibérico. In: Vera J.A. (Ed.) - Geología de España: 354-361. Sociedad Geológica de España-Instituto Geológico y Minero de España (SGE-IGME), Madrid.

Vegas R., de Vicente G., Casas-Sainz A. & Cloetingh S.A.P.L. (2019) - Alpine orogeny: intraplate deformation. In: Quesada C. & Oliveira J.T. (Eds.) - The Geology of Iberia: A Geodynamic Approach. The Alpine Cycle (Vol. 3): 507-518. Springer, Berlin. https://doi.org/10.1007/978-3-030-11295-0_12

Vergés J., Kullberg J.C., Casas-Sainz A., de Vicente G., Duarte L.V., Fernàndez M., Gómez J.J., Gómez-Pugnaire M.T., Jabaloy Sánchez A., López-Gómez J., Macchiavelli C., Martín-Algarra A., Martín-Chivelet J., Antón Muñoz J., Quesada C., Terrinha P., Torné M. & Vegas R. (2019) - An introduction to the Alpine Cycle in Iberia. In: Quesada C. & Oliveira J.T. (Eds.) - The Geology of Iberia: A Geodynamic Approach. The Alpine Cycle (Vol. 3): 1-14. Springer, Berlin. https://doi.org/10.1007/978-3-030-11295-0_1

White J.D.L. & Houghton B.F. (2006) - Primary volcaniclastic rocks. *Geology*, 34(8): 677-680. https://doi.org/10.1130/g22346.1

White J.D.L., Smellie J.L. & Clague D.A. (2003) - Introduction: A deductive outline and tropical overview of subaqueous explosive volcanism. In: White J.D.L., Smellie J.L. & Clague D.A. (Eds.) - Explosive subaqueous volcanism. Geophysical Monograph Series 140: 1-23. American Geophysical Union, Washington, DC. https://doi.org/10.1029/140gm01